Ref.TH.1343-CERN

PHENOMENOLOGY AT INTERMEDIATE ENERGIES *)

Christoph Schmid
CERN - Geneva

A B S T R A C T

The following topics are discussed. Regge features are more easily and more clearly seen at intermediate energies (shrinkage, polarization structure in t). The direct (local) confrontation of Regge and phase shift amplitudes in K^+p scattering. The partial wave analysis of the imaginary part of the non-flip amplitude in $K^\pm p$ elastic scattering and the problem of the strength of the low partial waves. The new interference model as a tool above the phase shift region. Moravcsik's phase band method. Semi-local duality in K^-p backward scattering and the qualitative difference between K^+p and K^-p at intermediate angles.

---

*) Invited talk at the Conference on the Phenomenology of Particle Physics, California Institute of Technology, March 25, 26 1971.

Ref.TH.1343-CERN
9 June 1971

1. - THE SIGNIFICANCE OF INTERMEDIATE ENERGY EXPERIMENTS FOR REGGEOLOGY

1.1. - Where does Regge start ?

It is surprising that simple Regge type features persist down to low energies in many reactions. As an operational definition for the beginning of the Regge region we require that the fluctuations in s at fixed t are quite small, say $\delta A/A \lesssim 15\%$.

A - In near forward elastic scattering, Regge features persist down to $p_{lab} \approx 1.5$ GeV/c. This came as a surprise to the CERN-Holland group [1]. They set out to discover Y^* resonances in $K^-p - K^-p$ in the region $p_L = 1.5 - 2.5$ GeV/c by measuring the polarization. Instead they found surprising Regge type regularities : they observed a dip at $t \approx -0.8$ GeV^2, whose position is pretty much independent of p_{lab} ; similarly the position of the first zero in the polarization is at $t \approx -0.8$ GeV^2 for all energies in the interval.

The new Argonne data [2] on the full angular distribution for the π^+p polarization at $p_L = 1.8 - 2.3$ GeV show, for $|t| \lesssim 1.5$ GeV^2, a great similarity to the polarization at higher momenta, Fig. 1. In fact the FESR Regge fit of Barger and Phillips [3] gives a good description for $|t| \leq 2.0$ GeV^2 and $p_L \geq 2.1$ GeV/c.

B - .In inelastic reactions, we have to distinguish between amplitudes where the low energy resonances add and those where the resonances cancel. The former type of amplitude is big and shows small fluctuations, the latter type is small and shows big fluctuations. An example for the former type is the spin-flip amplitude of π^-p CEX, for the latter type the non-flip π^-p CEX. Where we can isolate the latter type, as in $\sigma_{tot}(\pi^-p) - \sigma_{tot}(\pi^+p)$, we observe strong fluctuations up to $p_L = 2.5$ GeV/c. Where the former type dominates, as in $d\sigma/dt$ $(\pi^-p$ CEX) for $t \neq 0$, no s dependent (resonance type) structure is seen above $p_L \gtrsim 2.0$ GeV (with the present accuracy).

C - In πN backward scattering, one observes dramatic dips in $\sigma(180^{\circ})$ at $p_L \approx 2.1$ GeV/c for π^+p, π^-p and π^-p CEX. The $\Delta(11/2^+, 2420)$ at $p_L = 2.6$ still appears as a marked peak and the π^+p polarization at 2.75 GeV/c [2] looks qualitatively very different from the new results at 6 GeV [4]. Therefore Regge type experiments in the backward peak should not be done below $p_L = 4.0$ or 3.5 GeV/c. An exception is the exotic channel $K^+p - K^+p$. According to exchange degeneracy the backward peak should be purely real, and the polarization should vanish. Within statistical errors this is the case down to momenta as low as $p_L = 1.80$ GeV/c, see Fig. 2 [5].

1.2. - Regge shrinkage

Regge shrinkage is dramatic at large t, (say, $|t| \sim$ $\sim$ 1-3 GeV^2), see the π^+p data [6] in Fig. 3, and the effective trajectory in Fig. 4.

- The conclusion for the experimentalist : Regge features are more dramatic at large t, and in the past the gross structure in t over a large t interval has been more illuminating than fine details near t = 0.
- The conclusion for the theorist : the present cut models (weak or strong) fail badly beyond $|t| \sim 0.5$ GeV^2, they do not reproduce the strong shrinkage exhibited by the data, Fig. 4. One of the important tasks is to find a reasonable cut model for beyond $|t| \sim 0.5$ GeV^2.

Regge shrinkage is also observed for π^+p backward scattering in the intermediate energy region, $3.25 \leq p_L \leq 5.25$ GeV/c, see Fig. 5 from Ref. 7).

Plots of $\alpha_{effective}$ can be misleading, if the cross-section is a sum of several terms (particularly if there is destructive interference). It is cleaner to isolate a single term, e.g., $[d\sigma/dt(K^-p) - d\sigma/dt(K^+p)]$ in a pole model is the interference term between the

Pomeron and the vector mesons (ω, ρ). Therefore it should follow a simple power law $s^{\alpha_P+\alpha_M-2}$. In Fig. 6, Ref. 8), we see that the data follow such as a simple power law from $p_L = 15$ GeV/c all the way down to $p_L = 1.5$ GeV/c. Note particularly $|t| = 0.5 - 0.8$ GeV^2, where the statistics for the difference are good. The fitted exponent $n = \alpha_P + \alpha_M$ is shown on Fig. 7. We see that the shrinkage is even somewhat stronger than $\alpha'_P = 0.3$ and $\alpha'_M = 0.9$ GeV^{-2}.

1.3. - Structure in t

Regge experiments at large t, $|t| \approx 1.0 - 3.0$ GeV^2, are also important, because they teach us something about the qualitative behaviour of the amplitudes near the points $\alpha = 0, -1, -2$.

The qualitative features of the elastic $K^{\pm}p$ and $\pi^{\pm}p$ polarizations are simply explained by exchange degeneracy. The polarization arises from a Pomeron-meson interference.

Assuming the Pomeron to be purely imaginary, non-flip and without structure in t, the polarization becomes proportional to Re B_{meson}. Exchange degeneracy implies that the phase of the combined meson poles is $-e^{-i\pi\alpha}$ for K^-p, -1 for K^+p and $+1-e^{-i\pi\alpha}$ for the ρ term. Therefore the polarization is

$$\text{Pol.} \sim -\text{Re}\, B_{meson} \sim +1 \quad \text{for } K^+p$$
$$\sim +\cos\pi\alpha \quad " \quad K^-p$$
$$\sim +1-\cos\pi\alpha \quad " \quad P\sigma(\pi^+p) - P\sigma(\pi^-p)$$

This correctly gives the structure shown in Fig. 8, Refs. 9), 10) : the rise $\sim t^{\frac{3}{2}}$ of K^-p near $t = 0$, the comparable magnitude and positive relative sign of $K^{\pm}p$ near $\alpha = 0$, the zero of K^-p near $\alpha = -\frac{1}{2}$, the comparable magnitude and opposite sign for $K^{\pm}p$ near $\alpha = -1$, the

zero of $K^- p$ near $\alpha = -1.5$. In $\pi^\pm p$ it gives the well-known double zero of the difference of the polarization at $\alpha = 0$. Note that the low energy experiments ($K^\pm p$ at 2.7 GeV, $\pi^\pm p$ at 5 GeV) were more useful to Regge phenomenology than the experiments at higher momenta (available at that time), because the former covered a larger t interval with better statistics.

1.4. - Why experiments at intermediate energy ?

Because of interesting structure in t and because of dramatic Regge shrinkage at large t, experiments in the range $|t| \sim 1 - 3$ GeV^2 are important. But statistics becomes a problem at large t, therefore the experimentalist is forced to do Regge experiments at intermediate energies. Luckily, Regge features persist down to low energies (see 1.1). For elastic scattering and $|t| \lesssim 2.0$ GeV^2 one can do Regge experiments at a momentum as low as $p_L = 2.5$ or even 2.0 GeV/c.

It is a widely held misconception that Reggeology is "purest" and "simplest" at very small t and at the highest available energies. The last few years have taught us the opposite ; we must not close our eyes at the dramatic schrinkage at large t and at the beautifully simple large t structure of the polarization.

One might wonder whether Regge phenomenology will look very different at 70 - 500 GeV from 2 - 5 GeV. This is quite possible ; the relative importance of cuts may be very different. If at some future time there would be two simplified formulations, one useful and simple for 2 - 20 GeV, the other one for 20 - 200 GeV, then it would be the former which would be relevant for duality. The interlocking via FESR of the resonance region with the Regge region refers more to the intermediate energy Regge description than to the very high energy models.

2. - THE CONFRONTATION OF THE REGGE DESCRIPTION WITH THE PHASE SHIFT DESCRIPTION IN K^+p SCATTERING

K^+p scattering is a good place to compare directly (locally) the Regge and the phase shift descriptions. At fixed t, the data $(d\sigma/dt,\ P)$ for K^+p appear Regge behaved down to $p_L \approx 1.4$ GeV. On the other hand, phase shifts exist up to $p_L = 2.5$ GeV.

At each energy and momentum transfer, the present experiments give us only two quantities $d\sigma/dt$ and P. How is it possible to determine all four quantities, Re and Im of non-flip and flip ?

The crucial hypothesis for a phase shift analysis is that all partial waves above ℓ_{max} are either zero or fixed as a theoretical input (from partial wave dispersion relations or from Veneziano). If σ_{tot} and all moments A_n (of $d\sigma/d\Omega$) and B_n (of $P\, d\sigma/d\Omega$) up to $n = 2\ell_{max}$ are experimentally well determined, one has the same number of unknowns and of equations, namely $2\,(2\ell_{max}+1)$. In principle this allows us to arrive at the knowledge of four quantities at each energy and momentum transfer. Unfortunately, almost all equations are quadratic, and one is faced with an enormous ambiguity problem ; there are of the order of $2^{2L_{max}+1}$ solutions [11].

In a Regge model the phase of an amplitude can be obtained from the s dependence of the absolute magnitude of this amplitude. This allows us to arrive at the knowledge of three quantities at each energy and momentum transfer. The fourth quantity can never be determined in a Regge framework, because (for t not near zero) one can always rotate a Regge solution in the $a-b$ plane (spin non-flip/spin flip plane) without changing cross-sections or polarizations [for details, see Ref. 12].

In a confrontation between phase shifts and Regge, one must compare this third quantity, which can be defined as the "effective phase" :

$$\tan\varphi \equiv \left[\frac{(\mathrm{Im}\, a)^2 + (\mathrm{Im}\, b)^2}{(\mathrm{Re}\, a)^2 + (\mathrm{Re}\, b)^2} \right]^{1/2}$$

where a and b are t channel helicity amplitudes with kinematical factors absorbed such that $d\sigma/dt = |a|^2 + |b|^2$ and $Pd\sigma/dt = -2\,\mathrm{Im}(ab^*)$. It is useful to define the third quantity also in another way, which is equivalent, if $d\sigma/dt$ and P are measured (and fitted) at one given (s, t) with infinite accuracy. One considers the a - b plane (non-flip - flip plane) and draws the vectors $\vec{Re}$ = (Re a, Re b) and $\vec{Im}$ = (Im a, Im b). The angle between the two vectors, $\vartheta(\vec{Re}, \vec{Im})$, is this second possibility to define the third quantity.

In Fig. 9, such a comparison is made for K^+p scattering at p_L = 1.45 GeV/c. The solid lines show the predictions of various phase shift solutions [13),14)] for two possible (equivalent) definitions of the third quantity. We see that the various phase shift solutions strongly disagree among each other, although they look quite similar on the Argand plots. For example, at $t = -1$ GeV^2, the solutions have φ values from 20° (predominantly real) to 60° (predominantly imaginary). Some solutions tend to $\varphi \approx 90°$ (purely imaginary) towards the backward direction, in contradiction with the exchange degeneracy prediction that K^+p backward scattering should be purely real (and therefore P = 0, see Fig. 2).

The dots show the predictions of the effective pole model of Daum et al. [12)]. An effective pole model was chosen because the presently available cut models fail badly if one goes out to $|t| = 1.5$ GeV^2, e.g., they cannot reproduce the dramatic shrinkage shown by the data, Fig. 7, while our effective three-pole model gives quantitative fits. We see

on Fig. 9 that the Regge predictions strongly discriminate against the solutions ANL II, III, IV. They disfavour the solutions ANL I, CERN α, γ, while the agreement is moderate with CERN β.

We conclude that in principle the Regge approach allows us to discriminate among phase shift solutions. What is now needed are Regge models which are quantitatively reliable out to 1.5 GeV^2.

3. - THE GEOMETRICAL PICTURE

A useful "language" for the Reggeologist is to plot his amplitudes not versus t (at fixed p_{lab}) but versus ℓ or equivalently versus this impact parameter $b \equiv \ell/k$. In general a partial wave analysis at high energy requires reliable Regge amplitudes out to fairly large t as an input. In special cases, however, there are shortcuts, if one is willing to make certain approximations. Davier and Harari [15] use, for $K^{\pm}p$ elastic scattering at 5 GeV, the following approximations :

(i) neglect R^2 terms compared to P^2, but keep the interference terms $P \cdot R$, where P = Pomeron, R = ordinary Regge pole ;

(ii) assume the Pomeron to be purely imaginary for $t \neq 0$;

(iii) assume that R is purely real in K^+p since there are no resonances.

With these assumptions, one obtains :

$$d\sigma/dt\,(K^+p) \propto |P|^2$$

$$d\sigma/dt\,(K^-p) \propto |P|^2 + 2|P|\,\mathrm{Im}\,R_{\Delta\lambda=0}$$

In the differential cross-section, interference with P is only possible for that part of the R amplitude which has the same phase and spin structure as P (s channel helicity non-flip, $\Delta\lambda = 0$). Solving for $\mathrm{Im}\, R_{\Delta\lambda=0}$, we obtain

$$\mathrm{Im}\, R_{\Delta\lambda=0} = \frac{\frac{d\sigma}{dt}(K^-p) - \frac{d\sigma}{dt}(K^+p)}{2\sqrt{\frac{d\sigma}{dt}(K^+p)}}$$

$\mathrm{Im}\, R_{\Delta\lambda=0}$ is shown in Fig. 10. We see the well-known cross-over zeros at $|t| = 0.2$ and $1.3\ \mathrm{GeV}^2$. They are shifted (by cuts) compared to the positions in an exchange degenerate pole model, $\alpha(t) = 0, -1$.

The position of the first zero is simply connected (via FESR) to the first zero of the intermediate energy resonances. Helicity non-flip corresponds to an angular dependence $P_\ell(\cos\vartheta)$ while helicity flip corresponds to $P'_\ell(\cos\vartheta)$. Therefore the first zero in the non-flip amplitude must be closer to $t = 0$ than the first zero in the flip amplitude. This means that the exchange degeneracy of the t channel Regge amplitudes must be broken (by cuts), because of the spin structure of the direct channel resonances.

The curve drawn through the points in Fig. 10 is motivated by the picture of one dominant (band of) partial wave(s) containing the zeros of $P_\ell(\cos\vartheta)$ or of its asymptotic form $J_0(c\sqrt{-t})$. Since a fundamental feature of the difference plotted in Fig. 10 is the strong Regge shrinking shown in Figs. 6, 7, J_0 must be multiplied by a shrinkage factor $\exp[B(s)t]$. In partial wave language this means that one needs an expanding band (Δb) of impact parameters participating, i.e., we must have a collective effect of many partial waves.

Figure 11 shows the partial wave analysis of $\mathrm{Im}\, R_{\Delta\lambda=0}$ *). We see indeed a peaking for an impact parameter of about one fermi ; this means that the imaginary part of the ordinary Regge amplitude is a

---

*) It makes no sense to partial wave analyze differential cross-sections. What one analyzes here is the imaginary part of an amplitude (approximately). The result can be trusted for low and intermediate ℓ, but not for high ℓ.

peripheral effect. We also see that a broad band of partial waves is needed, $\delta \ell \approx 6$. At $p_{lab} = 5$ GeV the parent trajectory (Y_0^* : $\frac{1}{2}^+$, $\frac{3}{2}^-$, $\frac{5}{2}^+ \ldots$) is at $\ell = 10$, while the dominant partial wave, $\ell = kb \sim \sqrt{s}$, is at $\ell \approx 7$.

The unabsorbed Veneziano amplitude and the empirical amplitude in Fig. 11 have the common feature of a collective effect of many partial waves, from $\ell = \ell_{parent} \sim s$ down to $\ell = 0$. In both cases the partial waves which are dominant for $-1 < \cos\vartheta < +1$, are near $\ell = \ell_{dominant} \sim \sqrt{s}$. The difference lies in a strong suppression of the very low partial waves in the empirical amplitude ($\ell \lesssim 3$ at 5 GeV) compared to the unabsorbed Veneziano amplitude.

Veneziano models for KN, $\bar{K}N$ with weak or no absorption have the following feature : if fitted to $\sigma_{tot}(K^{\pm}p, K^{\pm}n)$, and with the flip - non-flip ratio from $d\sigma/dt$ (CEX) and from the assumption that ω-f decouple from s channel flip, one predicts the strength of the Y^* parent resonances too small by about a factor 2. This statement can be turned around : if the parent resonance strength is the input, then the forward amplitudes which are the sum of parents and all daughters, $\sum_{\ell} (2\ell + 1)\, a_\ell$, come out too large by about a factor 2. In other words the daughters must be absorbed more strongly. What is needed is a new absorption model which uses non-sense wrong signature zeros in the input (e.g., a Veneziano input) like the Argonne model, but which has stronger absorption in the very low partial waves than the Argonne model.

If one has a broad band of partial waves centered at ℓ_{dom}, the first (and in our case also the second) zero of the angular distribution will be given by the zero(s) of P_ℓ with $\ell = \ell_{dom}$. Further out in t there will be strong cancellations within the band of important waves in order to give the Regge shrinkage ; therefore the zeros are not expected to be given by the wave with $\ell = \ell_{dom}$. Experimentally the second and third ross-over zeros (at $|t| = 1.3$ and about 2.2 GeV^2) are approximately given by the exchange degeneracy positions, $\alpha = -1, -2$.

For pp and $p\bar{p}$ elastic scattering the second and third cross-overs disappear, $d\sigma/dt(p\bar{p})$ stays smaller than $d\sigma/dt(pp)$ after the first cross-over. In this case both the exchange degeneracy picture and the ℓ_{dom} picture (J_o picture) need important corrections.

Why is the scattering (at 5 GeV) strongest near an impact parameter of 1 fermi (see Fig. 11) ? The effective impact parameter is directly connected to the first zero of the angular distribution. This first zero occurs at a t value, which is independent of s, and which is the same for the Regge amplitude at 5 GeV and for the intermediate energy resonances. Therefore the dominant impact parameter is independent of s, and the value of 1 fermi is the value given by the intermediate energy resonances, $Y^*(\frac{5}{2}^{\pm}\ \frac{7}{2}^{\pm}\ \frac{9}{2}^{\pm})$.

In Fig. 12, we see that the Pomeron is mostly in low partial waves.

Only the imaginary part of the (non-Pomeron) Regge amplitude is peripheral. The real part is central in K^+n CEX, but peripheral in K^-p CEX. This comes from the Regge signature factors which give :

$$K^-p \text{ CEX} : -e^{-i\pi\alpha}$$

$$K^+n \text{ CEX} : -1$$

The slope of the forward peak is directly related to the average radius of interaction :

$$F(t) = C\, e^{\frac{1}{2}Bt}$$

$$\frac{1}{2}B = \frac{dF/dt}{F}\Big|_{t=0} = \frac{\sum_\ell (2\ell+1)\, a_\ell\, \frac{\ell(\ell+1)}{4q^2}}{\sum_\ell (2\ell+1)\, a_\ell} = \left\langle \frac{b^2}{4} \right\rangle$$

Predazzi [16] has plotted this experimental slope B of the forward peak for $\pi^+ p - \bar{\pi}^+ p$, as a function of energy, see Fig. 13. As we come to the $\Delta(\frac{7}{2}^+, 1920)$, the average radius of interaction shows a sharp increase. This is still another indication that intermediate energy resonances are peripheral effects.

There is a funny change of roles. A few years back, in the interference model, people thought that resonances correspond to central collisions and Regge exchanges correspond to peripheral collisions. Now we have seen that resonances are quite peripheral effects ($b \sim 1$ fermi) and that the unabsorbed Regge amplitude is not peripheral enough.

4. - THE NEW INTERFERENCE MODEL

Above the present phase shift region, $p_L \gtrsim 2.5$ GeV/c in πN, one still sees resonance structure, particularly in the backward direction. What model could be used to fit this region ? The Veneziano model is not flexible enough (in practice) to give quantitative fits, quite apart from the difficulties with treating fermions correctly. Therefore one considers a model with resonances plus "something else".

Duality assumes resonance saturation for the imaginary part, therefore the imaginary part is represented either by resonances or by Regge exchanges. In addition we have the Pomeron. While the usual duality framework is explicit about the imaginary part, it says little about the real part, which must be computed from dispersion relations. In this sense the $K^+ n$ charge exchange (CEX) amplitude, which is purely real, is built by the long range tails of the Y^* resonances in the crossed channel.

Before discussing the real part in more detail, let us look at the Indiana model [17]. They fit the $\pi^+ p$ backward peak as a sum of resonances only. The inconsistency of this ansatz is evident when applied to $K^+ p$ backward scattering. Since there are no (strong) $K^+ p$ resonances the Indiana approach would imply that there is no (strong) backward peak in $K^+ p$, while duality merely says that the imaginary part of the $K^+ p$ backward peak should be zero. Experimentally $K^+ p$ has a strong backward peak (Λ, Σ exchange), but the polarization is $0 \pm 20\%$ for $p_L = 1.6 - 2.3$ GeV/c (see Fig. 2), in agreement with the duality prediction.

A step forward in the treatment of the real part is the new interference model by Coulter, Ma and Shaw [18]. It is useful to consider separately the u channel and s channel resonances in the FESR :

$$\int_{-N}^{+N} \frac{\mathrm{Im} F_{res.}\, ds'}{s'-s} \approx \sum u \text{ reson.} + \sum s \text{ reson.} \qquad (4.1)$$

Similarly it is useful to split up the full Regge term not into even signature and odd signature parts, but rather into parts which have only either a s channel ($\cos\vartheta_t > +1$) or a u channel ($\cos\vartheta_t < -1$) cut :

$$\left[\mp 1 - e^{-i\pi\alpha(t)}\right] s^{\alpha(t)} = \mp s^{\alpha(t)} - (-s)^{\alpha(t)} \qquad (4.2)$$

(For definiteness we assume that we are in the s channel, s positive.) Duality (i.e., resonance saturation and Regge pole dominance) implies that we can either use both types of resonances or both types of Regge terms (in the absence of the Pomeron). But we note that there is a one-to-one correspondence between the splitting up into two terms in (4.1) and (4.2), e.g., the first terms in both expressions have no s channel discontinuities. The new interference model uses, when working in the

s channel, the second term of (4.1) and the first term of (4.2), i.e., they take the s channel resonances and add that part of the t channel Regge pole which has the discontinuity in the u channel *). In the Veneziano model, the decomposition looks as follows :

in the s channel : $V_{st} + V_{su}$ + V_{ut}

$V_{st} + V_{su}$: s resonances

V_{ut} : purely real Regge term

where V_{ut} has singularities in u and t only.

For the real part and the problem of tails this is quite a step forward, the tails of the u channel resonances are now neatly parametrized by the V_{ut} Regge term. We are still faced with the problem of the tails of low energy s channel resonances.

Yokosawa tries to circumvent this by using resonances only in the imaginary part and taking for the real part the full Regge real part. This is not good, because any s dependent structure in the imaginary part is reflected (via analyticity) in an equally important structure in the real part.

The problem of high energy tails of low energy resonances is intimately tied to the problem of daughter partial waves at intermediate energies. The necessity for daughters is obvious, because $|f(0^\circ)| \gg |f(180^\circ)|$. The backward amplitude is small because many (large) partial waves cancel against each other. There have been many fits which used (at any given energy) only a few parent partial waves (in the imaginary part). They could obtain fits to some small u

---

*) Practically this means dropping the term $e^{-i\pi\alpha}$ in the Regge signature factor.

interval, say $0 \leq |u| \leq 1$ GeV^2. These models would not be able to build up the large (non-Pomeron contribution to the imaginary part of the) forward peak.

The test question to ask for any calculation with the new interference model is the following : does it have enough daughter resonances to build up $\sigma_{tot} - \sigma_{tot}$ (Pom) ? Figure 14 [Ref. 19] shows that after subtracting all the established and half-established Y^* resonances from $\sigma_{tot}(K^-p)$, one is still 7 mb above $\sigma_{tot}(K^-p$, Pom) for $p_L = 1.5 - 3.0$ GeV/c. Since σ_{tot}(resonances) $\approx$ ≈ 5 mb at 2 GeV, the resonance amplitude must be more than doubled. If one sticks to the model, one needs a lot of new resonances for which there is not yet direct evidence. If one parametrizes the 7 mb difference as background, this background would correspond to the daughter partial waves of the ordinary Regge exchange, while the higher partial waves of Regge would correspond to the explicit resonances. Such an approach would be similar to the phase band method (discussed in Section 5), with the difference that here the background is parametrized in (s,t) with a simple s dependence, while there the parametrization is in ℓ (in the impact parameters) with little emphasis on the s dependence.

The best place to try out the new interference model is in those cases where at least one of the three ingredients (s resonances, u-t Regge term, Pomeron) is absent : (i) $\bar{K}N$ elastic scattering : Pomeron + resonances [20] ; (ii) $K^-p - \bar{K}^0n$: only resonances [19] ; (iii) $\pi^-p - \pi^0n$: resonances + u-t Regge term.

A consistent fit in the new interference model needs a lot of parameters, and in order to tie them down one must fit the full angular range of $d\sigma/d\Omega$ and P over a large energy interval. So we are almost back to an energy dependent phase shift analysis, with the exception that the background parametrization is more economical and physically more meaningful.

5. - THE PHASE BAND METHOD

Moravcsik has proposed another tool for analyzing data above the phase shift region [21]. He parametrizes the low partial waves, $0 \leq \ell \leq \ell'$, in a collective way (phase band), practically by cubic functions for $\delta(\ell)$ and $\eta(\ell)$. The high partial waves, $\ell' < \ell \leq \ell_{max}$, are parametrized individually as in the usual phase shift analysis, therefore they are allowed to contain resonances. The method has been applied by Bridges, Moravcsik and Yokosawa [22] to $\pi^+ p$ scattering at $p_L = 2.5$ and 2.75 GeV with $\ell' = 4$ and $\ell_{max} = 6$. It is now important to notice that there is not <u>one</u> phase band, but rather there are eight phase bands : we need a separate parametrization for $j = \ell + \frac{1}{2}$ and $j = \ell - \frac{1}{2}$, for even ℓ and odd ℓ, for Re and Im or equivalently for δ and η. If we have a cubic fit in each phase band we need $8 \times 3 = 24$ parameters, while the conventional analysis uses only $2(2\ell' + 1) = 18$ parameters. This means that one must go to much higher energies in order to make this method economical. Bridges et al. [22] halve their number of free parameters by not distinguishing even ℓ from odd ℓ.

One might ask whether it might be all right not to distinguish between even and odd ℓ nor between $j > \ell + \frac{1}{2}$ and $j = \ell - \frac{1}{2}$, or to put the real parts to zero, for low partial waves. All this corresponds to the assumptions : (i) that the low partial waves are dominated by Pomeron exchange, which is verified by Fig. 12, and (ii) that the non-Pomeron part in the low partial waves $\ell \leq \ell'$ is negligible compared to the non-Pomeron part in the high partial waves $\ell > \ell'$, which is certainly not true according to Fig. 11.

Also we know independently of the figure that it is impossible to build an ordinary Regge exchange (with shrinkage) out of only two partial waves at 2.5 GeV, one needs a collective effect of many. We conclude that we really need eight phase bands.

In $K^-p - K^-p$ there is no backward peak at intermediate energies, therefore it is reasonable to drop the distinction between even ℓ and odd ℓ in the phase band. (Even in the peripheral waves there is, in an average sense, no distinction between even and odd partial waves, since the peripheral resonances are exchange degenerate.) This reduces the phase band parameters by a factor of two and makes this reaction a preferred place to apply the method.

6. - K^-p BACKWARD SCATTERING

At high energy, $\bar{K}N - \bar{K}N$ backward scattering is an exotic reaction : the exchanged Regge pole would have to be a Z^* resonance which cannot be built from three quarks.

The new data of the CERN-Orsay-Paris-Stockholm collaboration [23] show that at $p_L = 5$ GeV the 180° cross-section for K^-p is very much suppressed compared to K^+p : $\sigma_{K^-p}(180^\circ) : \sigma_{K^+p}(180^\circ) \approx 1 : 100$, see Fig. 15. From $p_L = 1$ to $p_L = 5$ GeV, one has a steep falling off in $\sigma_{K^-p}(u=0)$. The point at 5 GeV may or may not indicate the beginning of a different power law (Regge cut ?). This suspicion is strengthened by the observation that the K^-p angular distribution has a backward peak of the same relative height and width as the K^+p backward peak, see Fig. 16. In our context here it is important that this effect is very small in absolute terms.

If the high energy reaction is exotic, the low-energy resonances Y^* should average to zero at fixed u according to FESR duality. Let us consider $K^-p - \bar{K}^0n$ backward scattering. For $p_L < 1.7$ GeV one observes a strong backward peak. We shall now show that this strong backward peak is consistent with duality. We must consider the amplitudes rather than the differential cross-section.

In Fig. 17 [from Ref. 24], we show the imaginary and real parts of the backward amplitude ; they perform a damped oscillation around zero. We have a semi-local cancellation involving resonances spaced by $\delta(m^2) = 1\ \text{GeV}^2$, as opposed to a local parent-daughter cancellation. Note that, e.g., near $p_L = 1$ GeV the $\Sigma(\frac{5}{2}^-)$ and $\Lambda(\frac{5}{2}^+)$ contribute with the same sign and that daughter contributions are rather unimportant in this case (the dashed curve for resonances qualitatively agrees with the full phase shift amplitudes).

The exotic behaviour in the Veneziano model, e.g., for $\pi^+\pi^- - \pi^+\pi^-$ backward scattering, is produced by an increasing overlap of subsequent resonance towers (semi-local cancellation) and not by a local parent-daughter cancellation. In fact the magnitude of the combined parent-daughter contribution is symmetric with respect to the point $t + \frac{1}{2} = u$, which is approximately the point $\vartheta = 90^\circ$. For instance, at $u = -0.5\ \text{GeV}^2$ the combined parent-daughter contribution is as large as the secondary forward peak at $t = -1.0\ \text{GeV}^2$. The crucial difference between $t = -1.0\ \text{GeV}^2$ (non-exotic) and $u = -0.5\ \text{GeV}^2$ (exotic) as s becomes large, is the alternating sign of subsequent resonance towers in the exotic case. It is only through an increasing overlap (increasing $m\Gamma$) that the exotic behaviour for u fixed ($u \neq 0$) and $s \to \infty$ is produced. Therefore the rate of decrease of the backward K^-p cross-section ($d\sigma/du \sim p_L^{-9}$) is intimately tied to the increase of resonance widths.

Let us now consider large angle scattering (between the forward and the backward peaks), Fig. 16, and see how duality gives us some understanding of the qualitative features. The angular distributions look very different for K^+p and K^-p at large angles, $+0.3 \geq \cos\vartheta \geq -0.7$, at 5 GeV : K^+p is quite flat in this angular range, while K^-p falls far below in a skew V shaped manner. At 90° we have $d\sigma/dt(K^-p) : d\sigma/dt(K^+p) \approx 1:40$, see Fig. 16. Let us study the one-term Veneziano model in the analogous case of $\pi^\pm\pi^+$ elastic scattering :

$$V = - \frac{\Gamma(1-\alpha_s)\,\Gamma(1-\alpha_t)}{\Gamma(1-\alpha_s-\alpha_t)}$$

The s channel is $\pi^+\pi^- - \pi^+\pi^-$ (non-exotic, like K^-p), the u channel is $\pi^+\pi^+$ (exotic, like K^+p). For $s \to \infty$ and $t + \frac{1}{2} = u$ ($\vartheta_s \approx 90^\circ$) we obtain

$$|V| \to e^{-s\log 2}\,\sqrt{2\pi}\; e^{-\frac{\pi}{2}\,\mathrm{Im}\,\alpha(s)}$$

and for $u \to \infty$ and $t + \frac{1}{2} = s$ ($\vartheta_u \approx 90^\circ$) :

$$|V| \to e^{-u\log 2}\;\sqrt{2\pi}\;\sqrt{u}$$

The crucial difference between the exotic channel, $\pi^+\pi^+$, and the non-exotic channel, $\pi^+\pi^-$, is the factor $\exp\left[-\frac{\pi}{2}\,\mathrm{Im}\,\alpha(s)\right]$ which comes from the alternating sign of successive resonance towers in $\pi^+\pi^-$ for fixed angle. As $\mathrm{Im}\,\alpha(s) \to \infty$ these towers overlap increasingly and cancel each other more and more. In $\pi^+\pi^+$ no cancellations can occur. This explains qualitatively why K^-p falls far below K^+p at large angles.

REFERENCES

1) C. Daum, F.C. Erné, J.P. Lagnaux, J.C. Sens, M. Steuer and F. Udo - Nuclear Phys. B6, 273 (1968) ;

S. Andersson, C. Daum, F.C. Erné, J.P. Lagnaux, J.C. Sens, C. Schmid and F. Udo - 1969 Stony Brook Conference, "Hign Energy Collisions", Gordon and Breach (1969).

2) G. Burleson, D. Hill, S. Kato, P.F.M. Koehler, T.B. Novey, A. Yokosawa, D. Eartly, K. Pretzl, B. Barnett, A. Laasanen and P. Steinberg - Phys.Rev.Letters 26, 338 (1971).

3) V. Barger and R.J.N. Phillips - Phys.Rev. 187, 2210 (1969).

4) H. Aoi, N.E. Booth, C. Caverzasio, L. Dick, A. Gonidec, Z. Janout, K. Kuroda, A. Michalowicz, M. Poulet, D. Sillou, C.M. Spencer and W.S.C. Williams - Phys. Letters 35B, 90 (1971).

5) B.A. Barnett, A.T. Laasanen, P.H. Steinberg, D. Hill, S. Kato, P.F.M. Koehler, T.B. Novey, A. Yokosawa, G. Burleson, D. Eartly and K. Pretzl - Phys.Letters 34B, 655 (1971).

6) B.B. Brabson, R.R. Crittenden, R.M. Heinz, R.C. Kammerud, H.A. Neal, H.W. Paik and R.A. Sidwell - Phys.Rev.Letters 25, 553 (1970).

7) R.A. Sidwell, R.R. Crittenden, K.F. Galloway, R.M. Heinz and H.A. Neal - Phys.Rev. D3, 1523 (1971).

8) C. Daum, C. Michael and C. Schmid - unpublished.

9) Ref. 1), for K^+p polarization see also Ref. 13).

10) C. Schmid - 1969 Erice Lectures, Academic Press (1970) ;

P. Sonderegger - 1969 Moriond Lecture, Orsay Report, unpublished.

11) A. Gersten - Nuclear Phys. B12, 537 (1969).

12) C. Daum, C. Michael and C. Schmid - Phys.Letters 31B, 222 (1970), and preprint in preparation.

13) M.G. Albrow, S. Andersson/Almehed, B. Bosnjakovic, C. Daum, F.C. Frné, Y. Kimura, J.P. Lagnaux, J.C. Sens, F. Udo and F. Wagner - CERN Preprint((Dec. 1970), to be published in Nuclear Phys.

14) S. Kato, P. Koehler, T. Novey, A. Yokosawa and G. Burleson - Phys.Rev.Letters 24, 615 (1970).

15) M. Davier and H. Harari - SLAC Preprint (1971).

16) Y. Hama and E. Predazzi - Sao Paolo Preprint

T. Lasinski, R. Levi Setti and E. Predazzi - Phys.Rev. 179, 1426 (1969).

17) R.R. Crittenden, R.M. Heinz, D.B. Lichtenberg and E. Predazzi - Phys.Rev. D1, 169 (1970) ;

P.G. Tomlinson, R.A. Sidwell, D.B. Lichtenberg, R.M. Heinz, R.R. Crittenden and E. Predazzi - Nuclear Phys. B25, 443 (1971).

18) P.W. Coulter, E.S. Ma and G.L. Shaw - Phys.Rev.Letters 23, 106 (1969).

19) C. Bricman, M. Ferro-Luzzi, J.M. Perreau, G. Bizard, Y. Declais, J. Duchon, J. Seguinot and G. Valladas - Phys.Letters 31B, 152 (1970).

20) T.A. Lasinski - Nuclear Phys. B29, 125 (1971).

21) M.J. Moravcsik - Phys.Rev. 177, 2587 (1969).

22) D. Bridges, M.J. Moravcsik and A. Yokosawa - Phys.Rev.Letters 25, 770 (1970) ; Erratum Phys.Rev.Letters 26, 155 (1971).

23) C. Baglin et al. (CERN-Orsay-Paris-Stockholm Collaboration) - to be published.

24) C. Bricman, E. Pagiola and C. Schmid - CERN Preprint D.Ph.II/Phys. 71-15 (1971).

FIGURE CAPTIONS

Figure 1 π^+p polarizations, Ref. 2). The Regge pole prediction is from Ref. 3).

Figure 2 K^+p polarizations, Ref. 5).

Figure 3 π^+p differential cross-sections, Ref. 6). $\theta_{cm} > 180^\circ$ is marked by a hatched area.

Figure 4 $\alpha_{eff}(t)$ for π^+p above $p_L = 2.5$ GeV/c from Ref. 6). The solid line represents a trajectory of slope 1 GeV^{-2} with the ρ intercept.

Figure 5 Effective trajectory for π^+p backward elastic scattering with $3.25 \leq p_L \leq 5.25$ GeV/c, from Ref. 7).

Figure 6 The difference of K^-p and K^+p differential cross-sections plotted against $\nu = \omega_L + t/4M$ for fixed t values between 0 and -1 GeV^2, from Ref. 8).

Figure 7 The Regge exponent $n(t) = \alpha_P(t) + \alpha_M(t)$ from the fits in Fig. 6. The solid line corresponds to $\alpha_P = 1 + 0.3\ t$ and $\alpha_M = 0.5 + 0.9\ t$; Ref. 8).

Figure 8 Polarizations for $K^\pm p$ elastic scattering at $p_L = 2.74$ GeV/c, Ref. 9).

Figure 9 Comparison of phase shift and Regge predictions for K^+p elastic scattering at $p_L = 1.45$ GeV/c against t. Solid lines are phase shift solutions α, β, γ of CERN, Ref. 13), and I - IV of Argonne, Ref. 14). The dots are the fixed t Regge predictions, Ref. 12).
(a) the effective phase φ defined in the text,
(b) the angle θ $(\vec{Re}, \vec{Im})$ in the non-flip/flip plane.

Figure 10 The experimental results for $\frac{1}{2}[d\sigma/dt(K^-p) - d\sigma/dt(K^+p)] \cdot [d\sigma/dt(K^+p)]^{-\frac{1}{2}} \approx \mathrm{Im}\, R_{\Delta\lambda=0}$ as a function of t at $p_{lab} = 5$ GeV, Ref. 15).

Figure 11 Legendre coefficients for the amplitude $\mathrm{Im}\, R_{\Delta\lambda=0}$ of Fig. 10. The dashed area between the two curves represents the uncertainty introduced by both statistical and systematic errors, Ref. 15).

Figure 12 Legendre coefficients for $\sqrt{d\sigma/dt(K^+p)} \approx P$ and for $\sqrt{d\sigma/dt(K^-p)} \approx P + \mathrm{Im}\, R_{\Delta\lambda=0}$, where Pomeron $\approx iP$.

Figure 13 The slope B of the forward peak for π^+p elastic scattering as a function of p_{lab}.

Figure 14 K^-p total cross-section as a function of the K^- lab. momentum. The dashed curve is the fit by resonances plus background, the solid curve is the background contribution, Ref. 19).

Figure 15 K^+p and K^-p differential cross-sections at $u = 0$ versus p_L. The new 5 GeV points are from Ref. 23).

Figure 16 K^+p and K^-p angular distributions at 5 GeV, Ref. 23).

Figure 17 The imaginary and real parts for $K^-p - \bar{K}^0n$ backward scattering. The full lines are computed from various partial wave analyses, the dotted lines correspond to resonances only, Ref. 24).

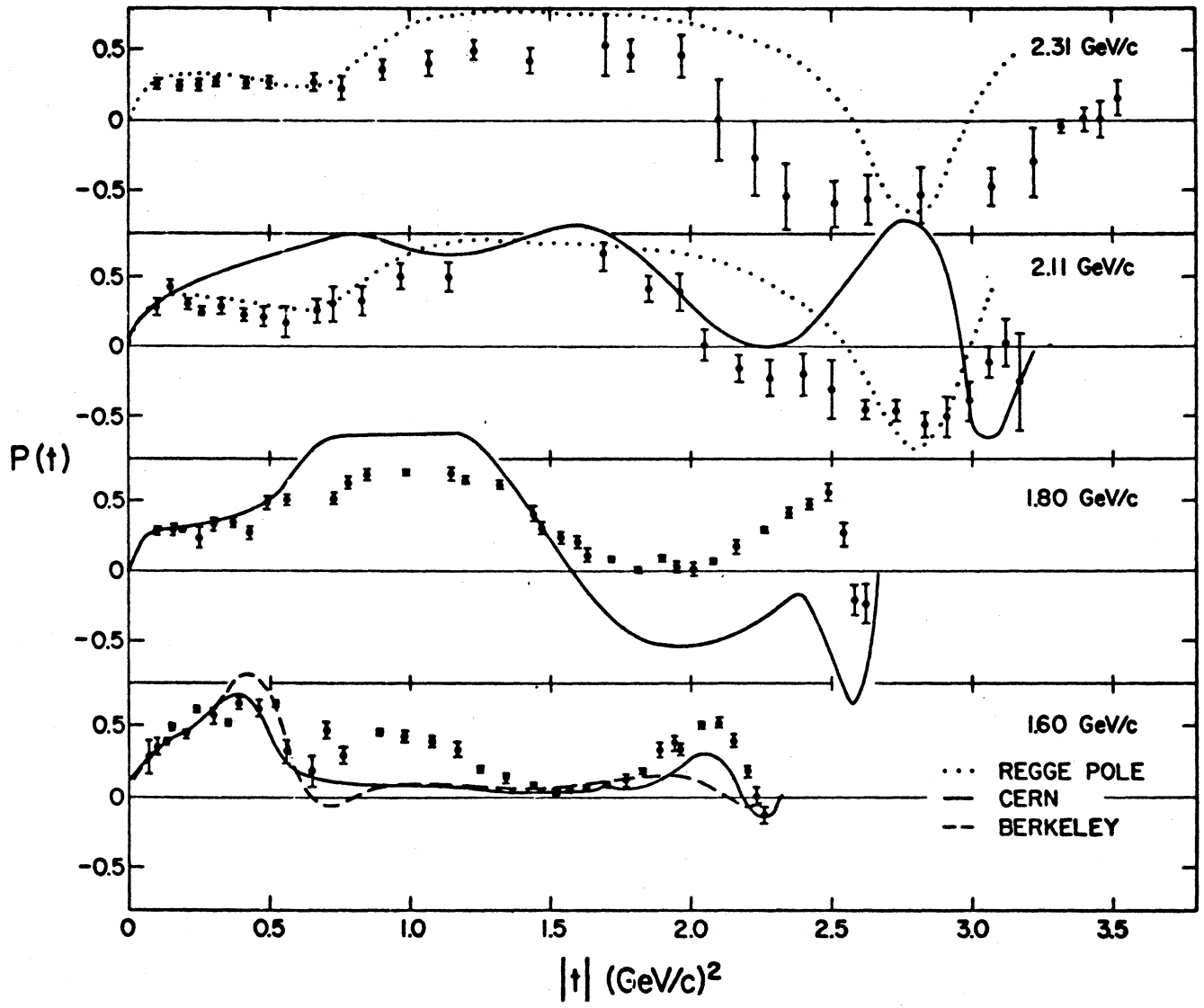
2.31 GeV/c
2.11 GeV/c
1.80 GeV/c
1.60 GeV/c
REGGE POLE
CERN
BERKELEY
P(t)
|t| (GeV/c)²
0.5
0
-0.5
1.0
1.5
2.0
2.5
3.0
3.5

FIG. 1

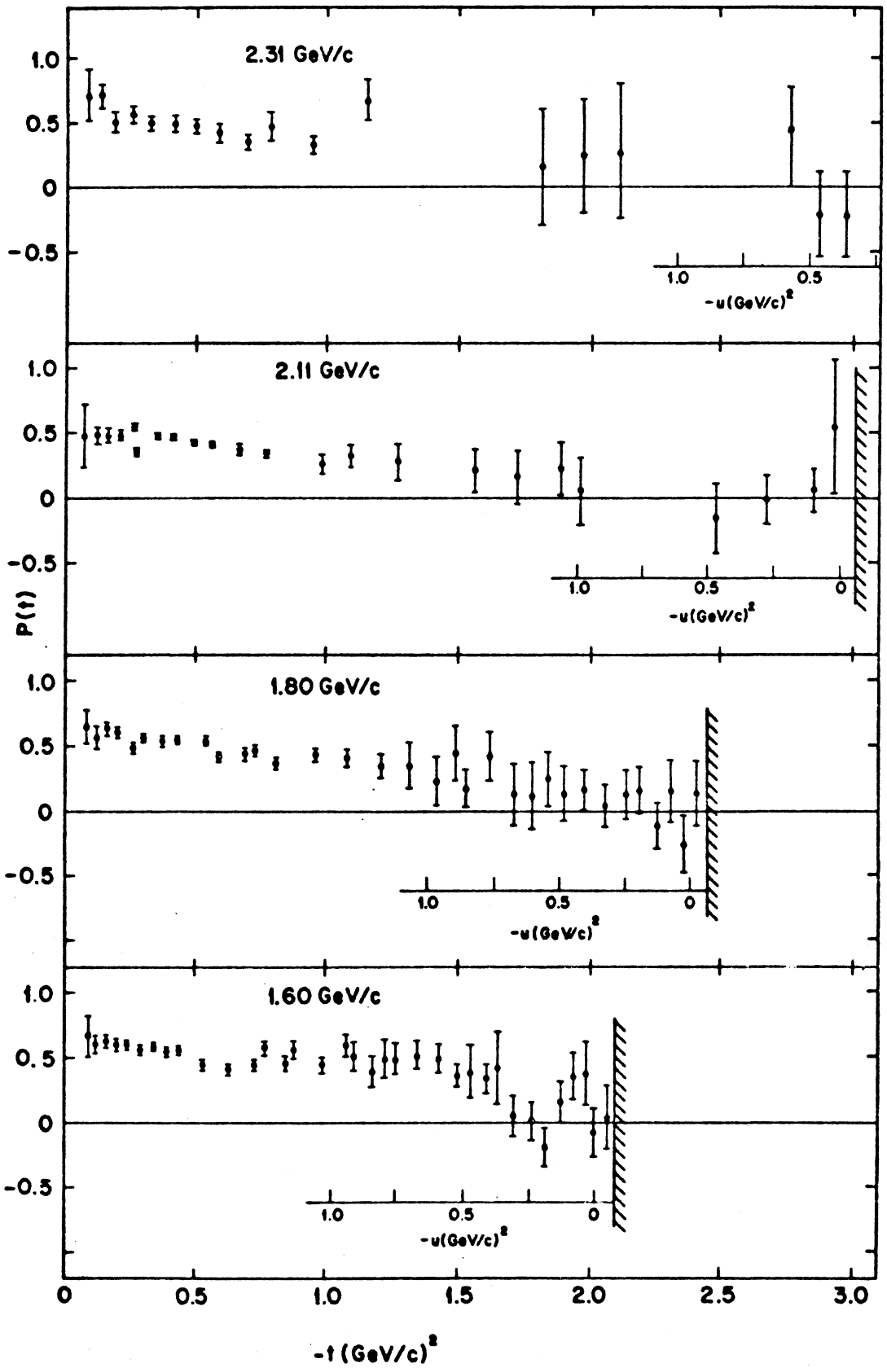

FIG. 2

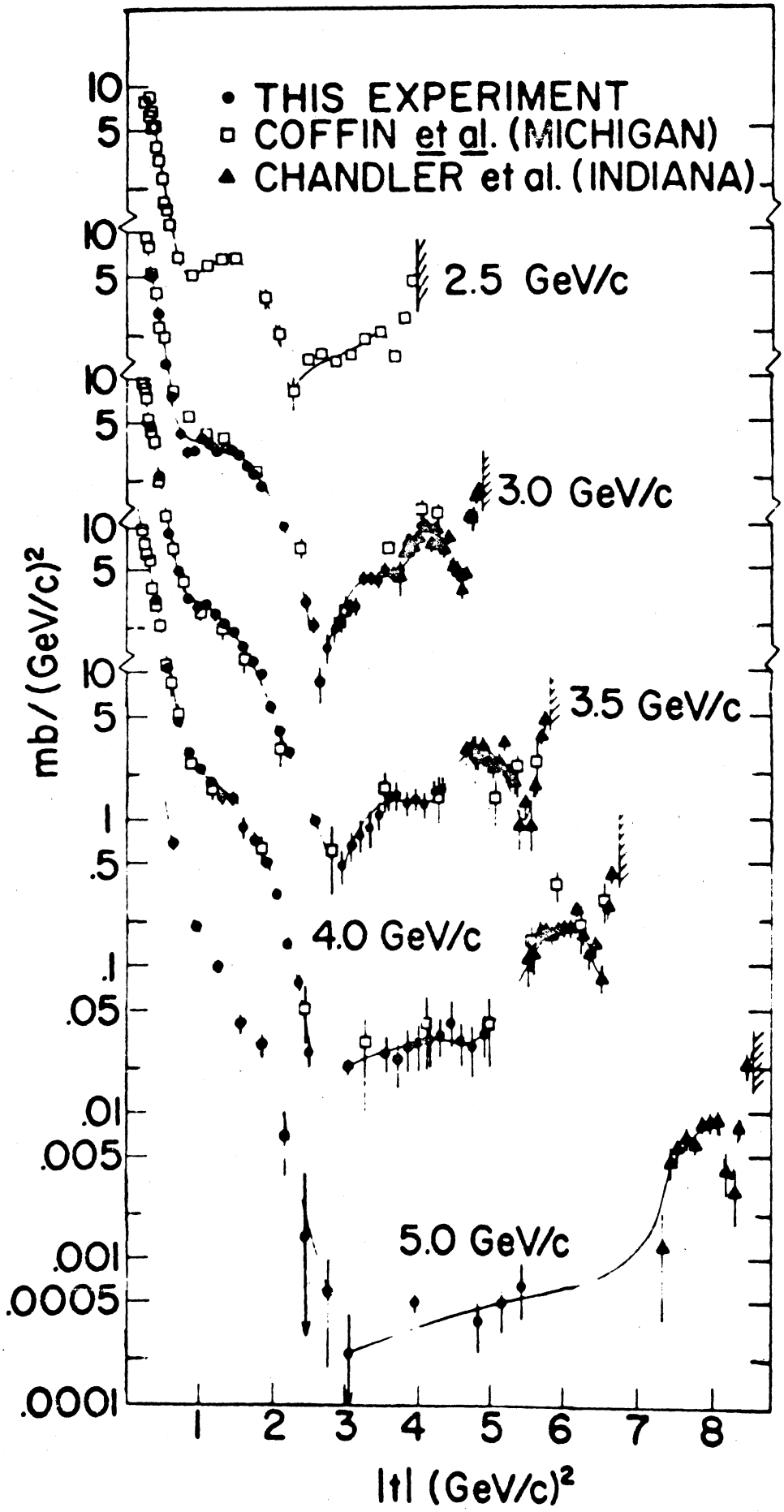
• THIS EXPERIMENT
□ COFFIN et al. (MICHIGAN)
▲ CHANDLER et al. (INDIANA)
2.5 GeV/c
3.0 GeV/c
3.5 GeV/c
4.0 GeV/c
5.0 GeV/c
mb/(GeV/c)²
|t| (GeV/c)²
10
5
1
.5
.1
.05
.01
.005
.001
.0005
.0001
1
2
3
4
5
6
7
8

FIG. 3

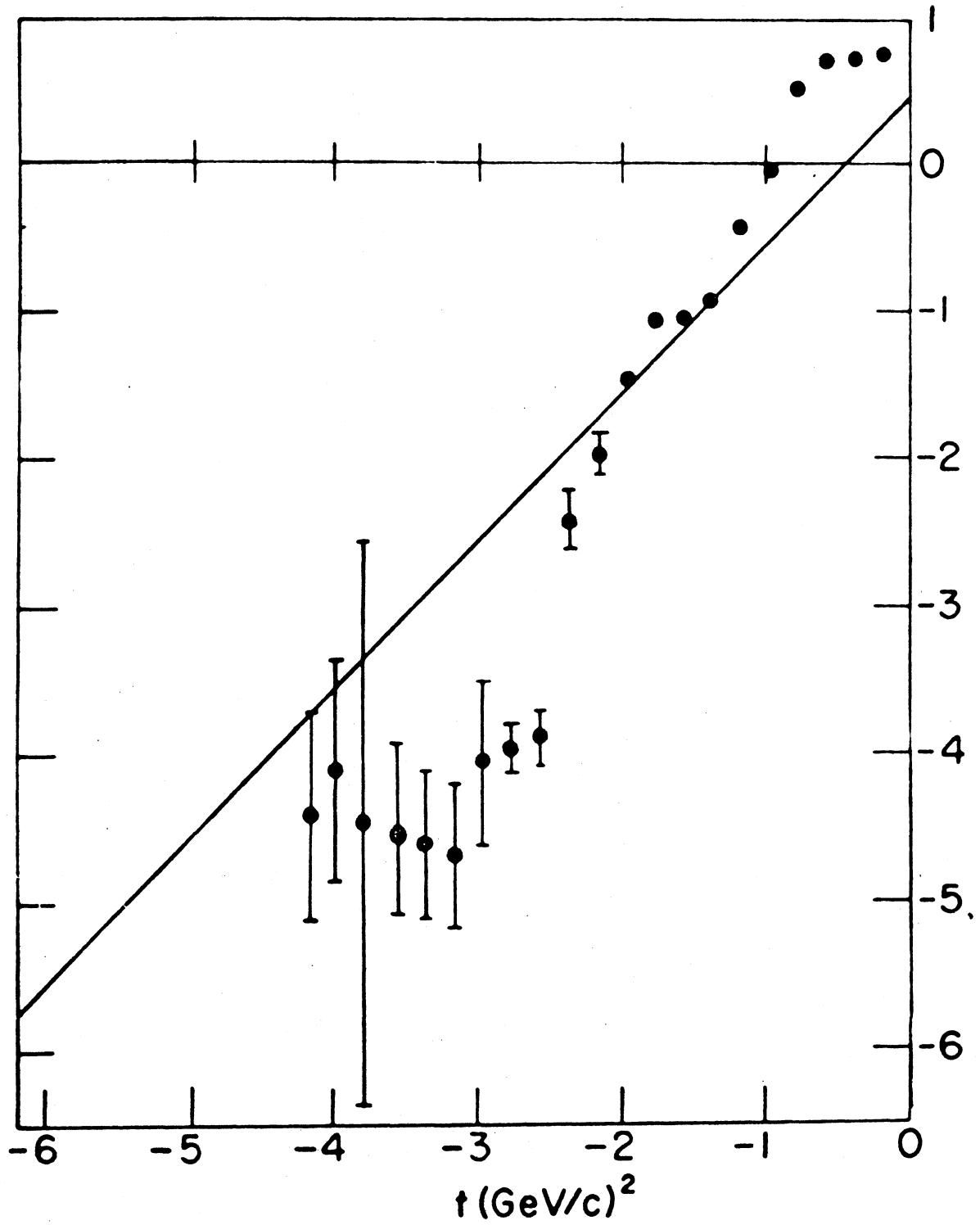

FIG. 4

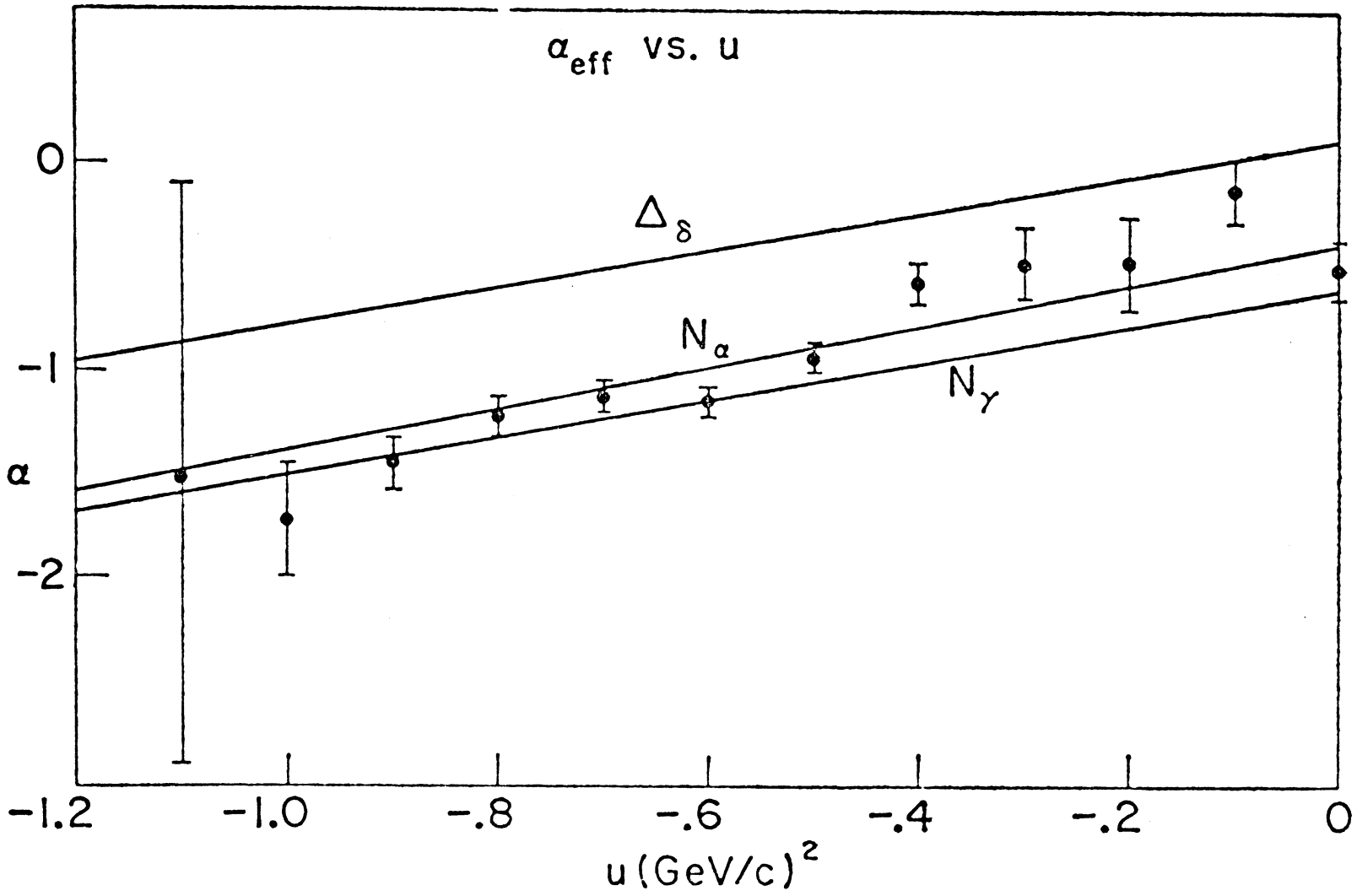
α_{eff} vs. u
0
-1
-2
α
Δ_δ
N_α
N_γ
-1.2
-1.0
-.8
-.6
-.4
-.2
0
u (GeV/c)^2

FIG. 5

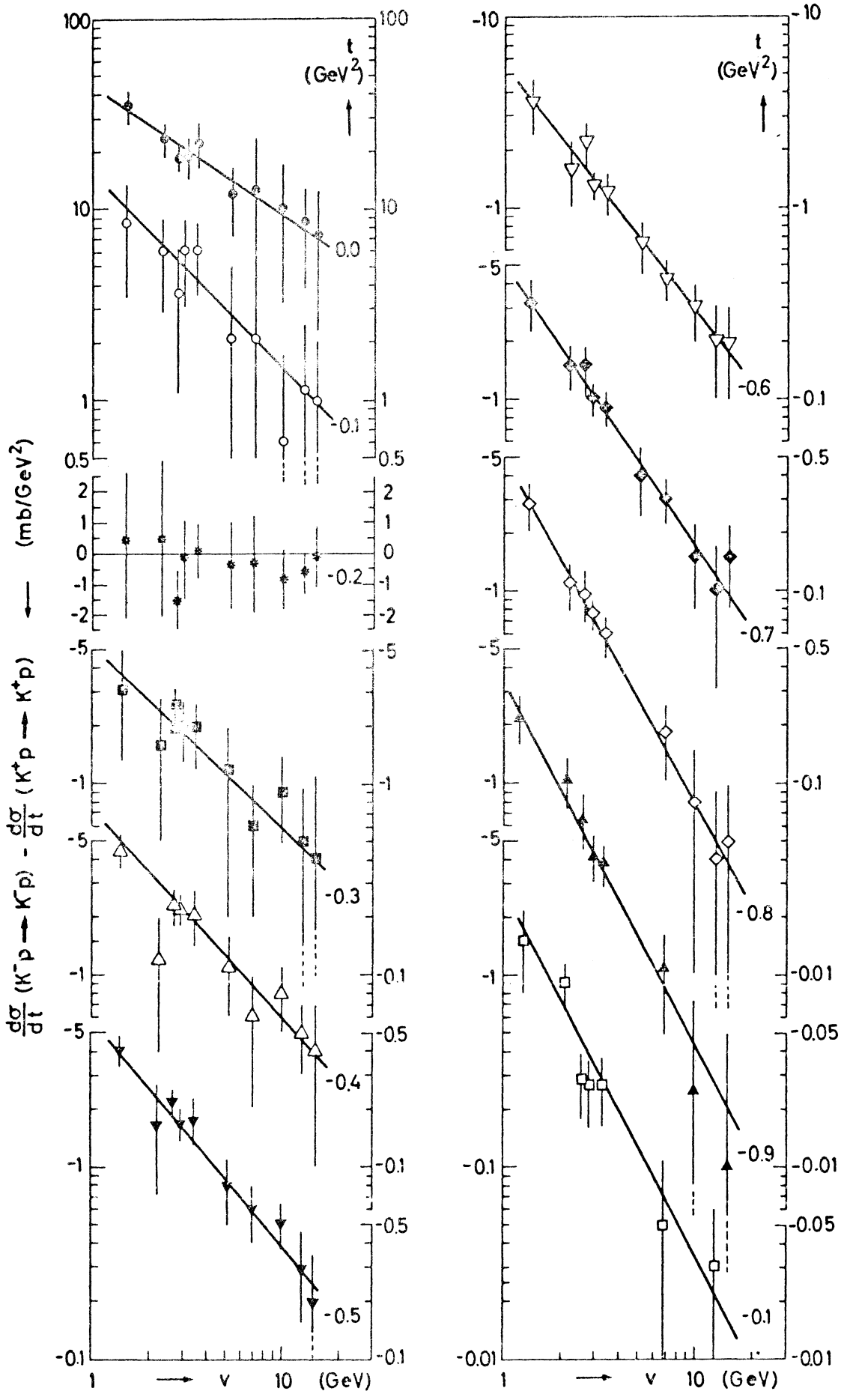
$\frac{d\sigma}{dt}(K^-p \to K^-p) - \frac{d\sigma}{dt}(K^+p \to K^+p)$ (mb/GeV^2)
t (GeV^2)
0.0
-0.1
-0.2
-0.3
-0.4
-0.5
-0.6
-0.7
-0.8
-0.9
-0.1
ν (GeV)
1
10

FIG. 6

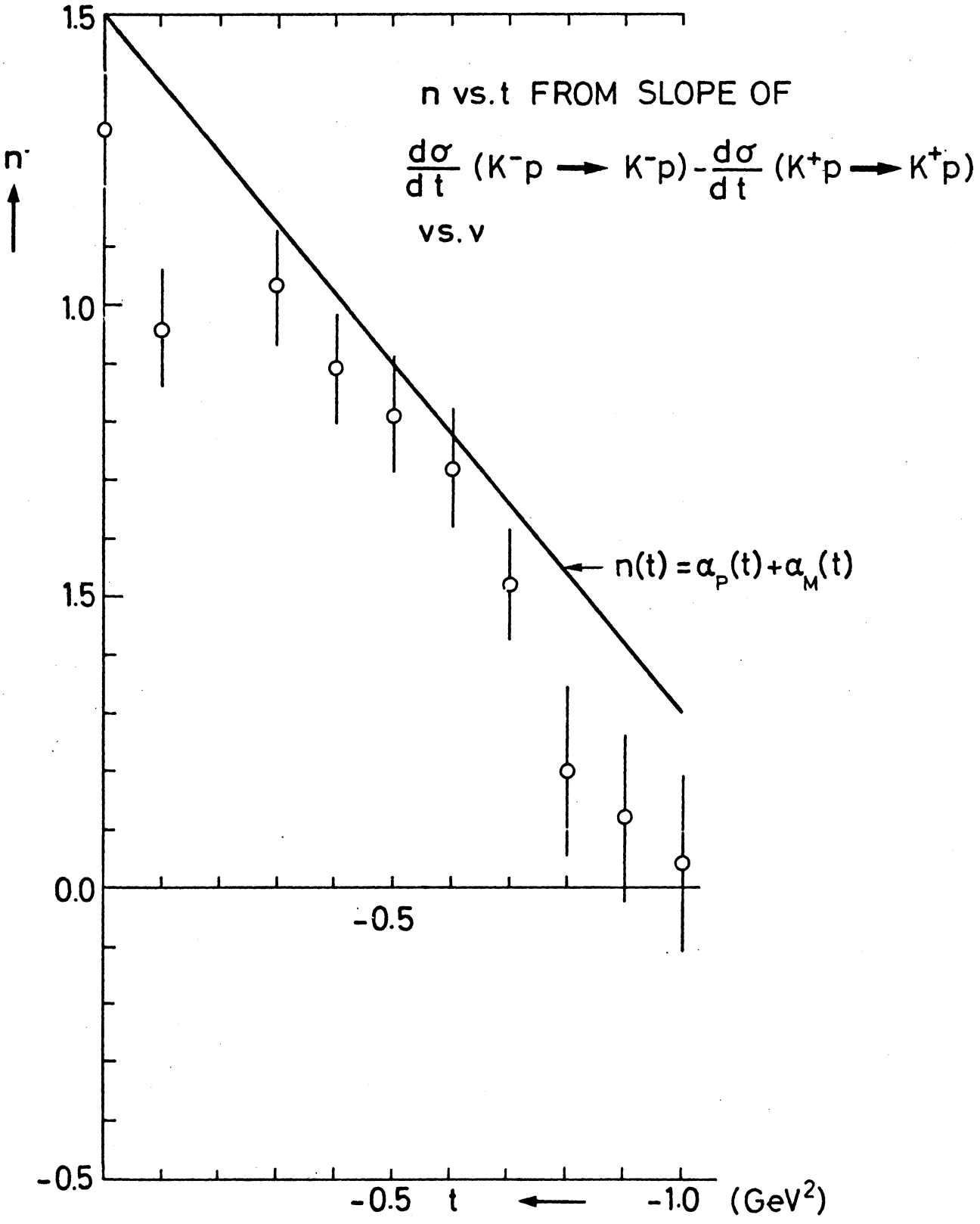
1.5
1.0
1.5
0.0
-0.5
n
n vs.t FROM SLOPE OF
$\frac{d\sigma}{dt}(K^-p \rightarrow K^-p) - \frac{d\sigma}{dt}(K^+p \rightarrow K^+p)$
vs. ν
$n(t) = \alpha_P(t) + \alpha_M(t)$
-0.5
-0.5
t
-1.0
(GeV^2)

FIG. 7

POLARISATION

KP ELASTIC SCATTERING 2.74 GeV/c

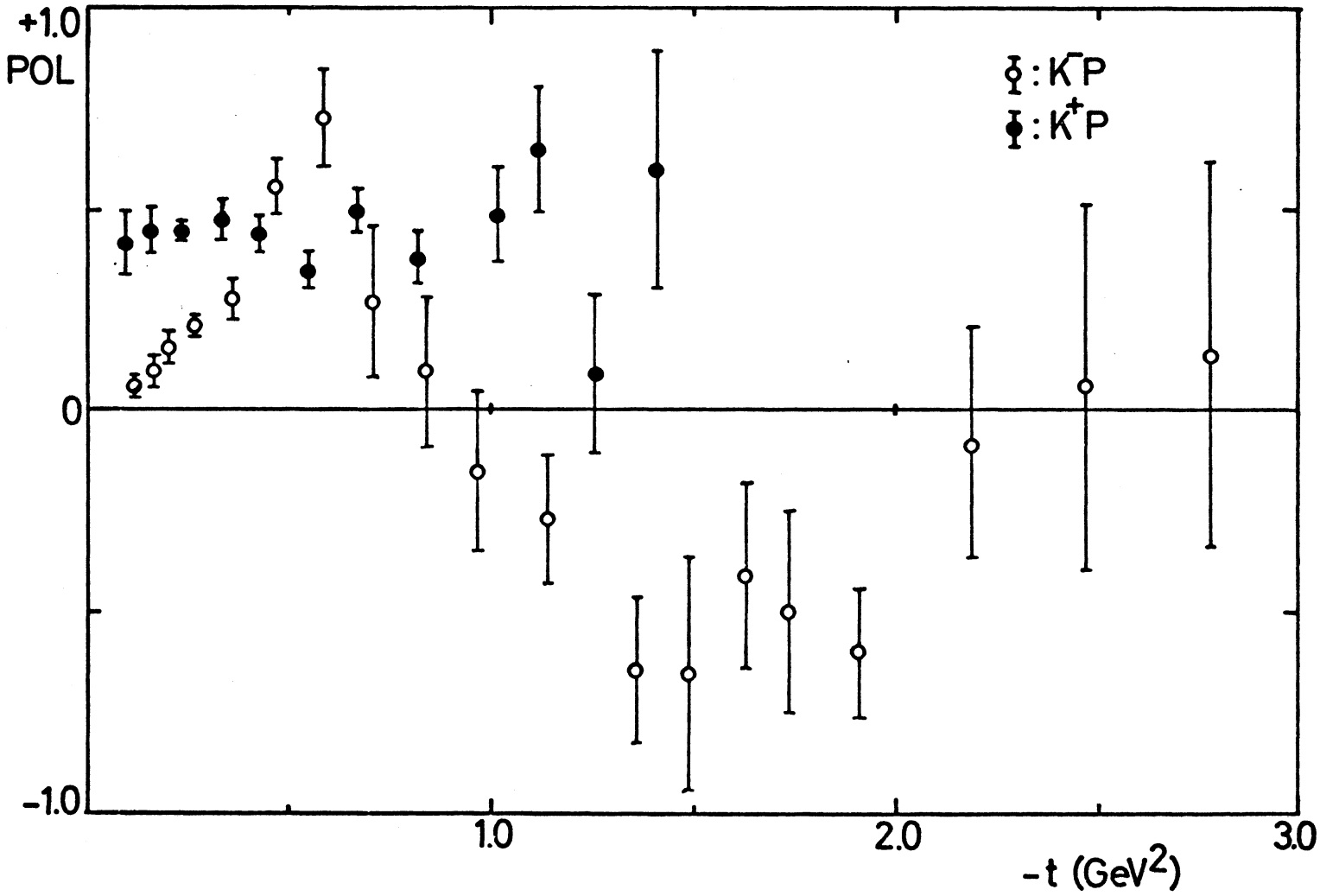

FIG. 8

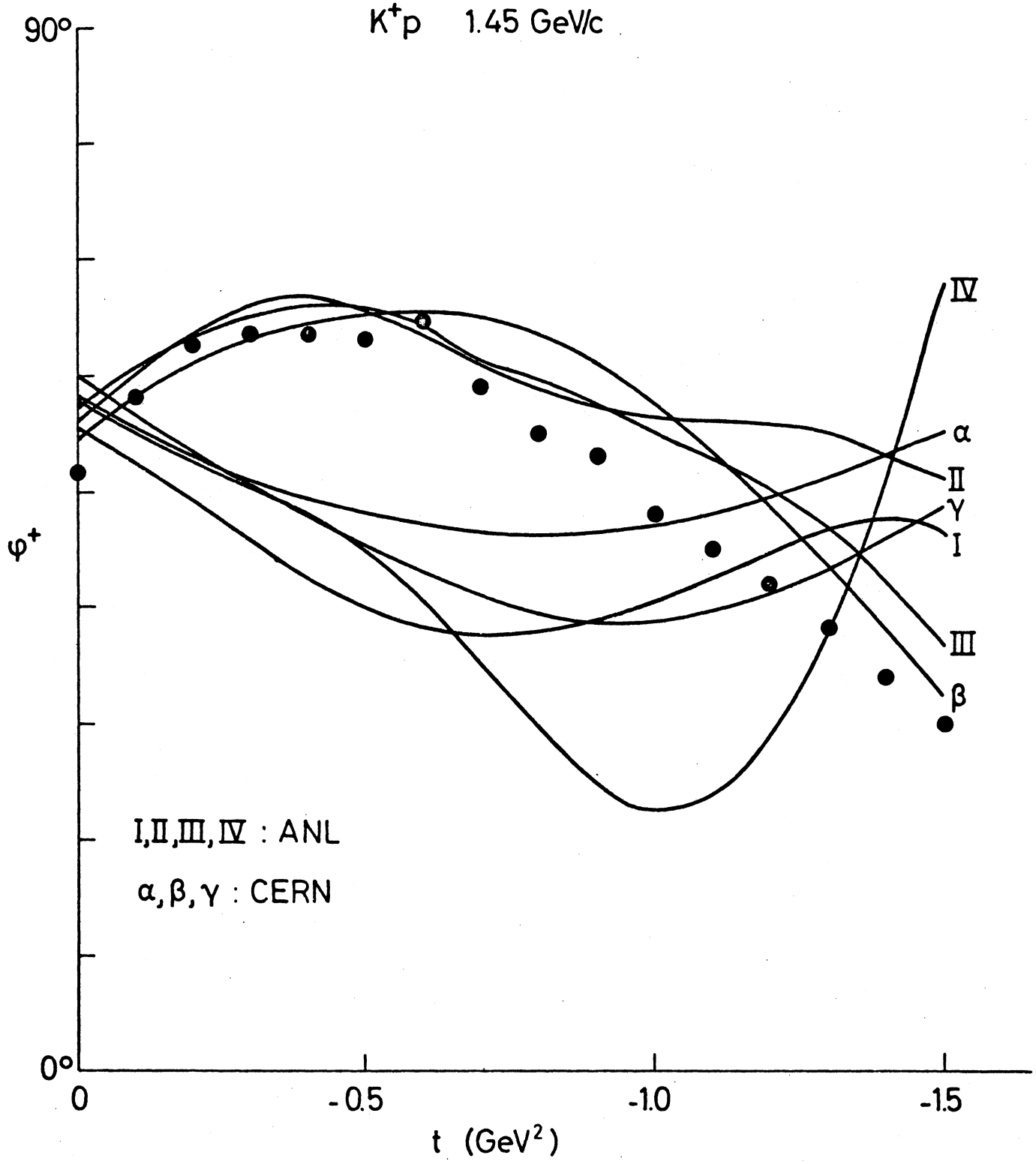
K^+p 1.45 GeV/c
90°
0°
φ^+
0
-0.5
-1.0
-1.5
t (GeV²)
I,II,III,IV : ANL
α,β,γ : CERN
IV
α
II
γ
I
III
β

FIG. 9a

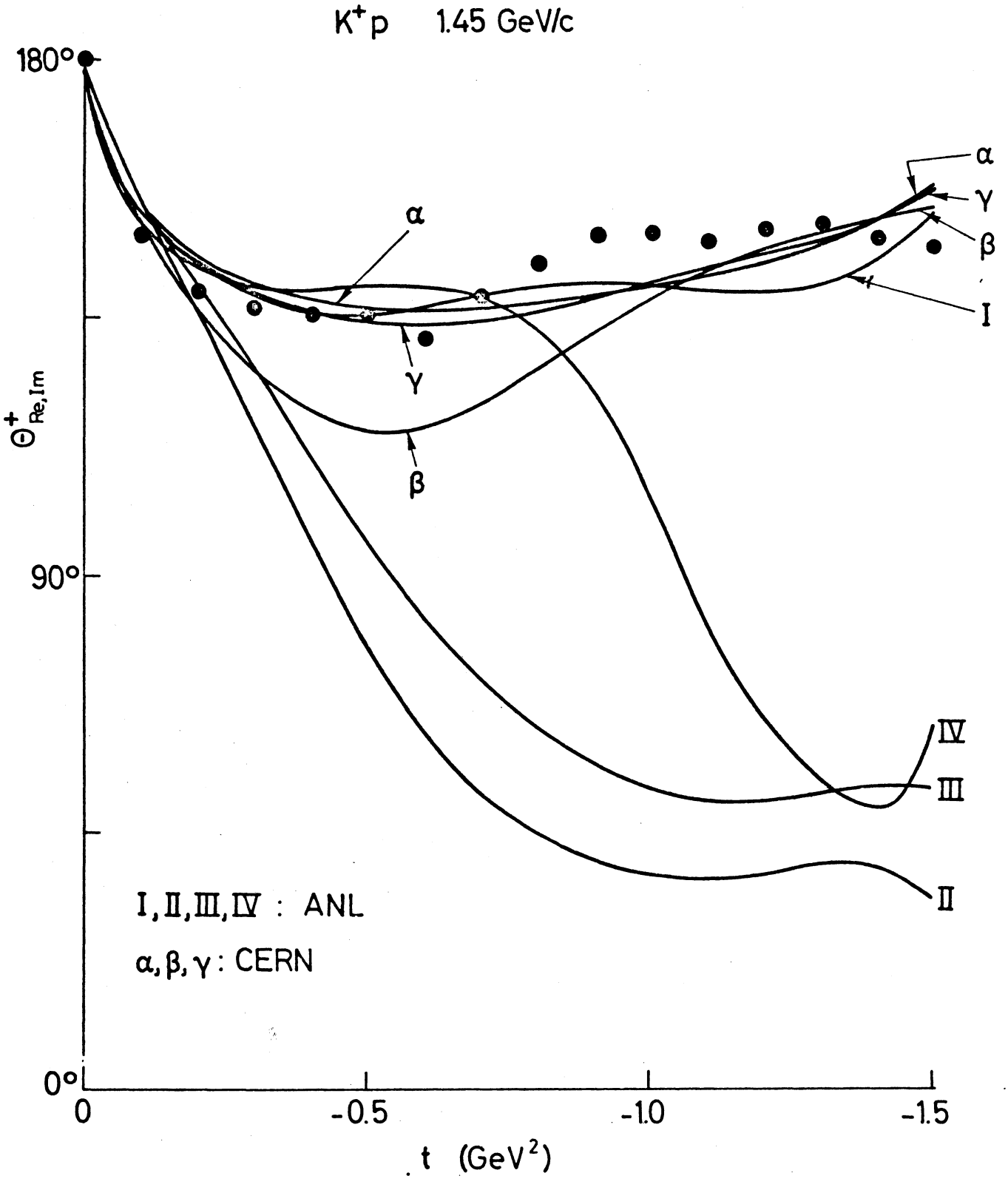
K+p 1.45 GeV/c
180°
90°
0°
0
-0.5
-1.0
-1.5
t (GeV²)
Θ+ Re,Im
α
γ
β
I
II
III
IV
I, II, III, IV : ANL
α, β, γ : CERN

FIG. 9b

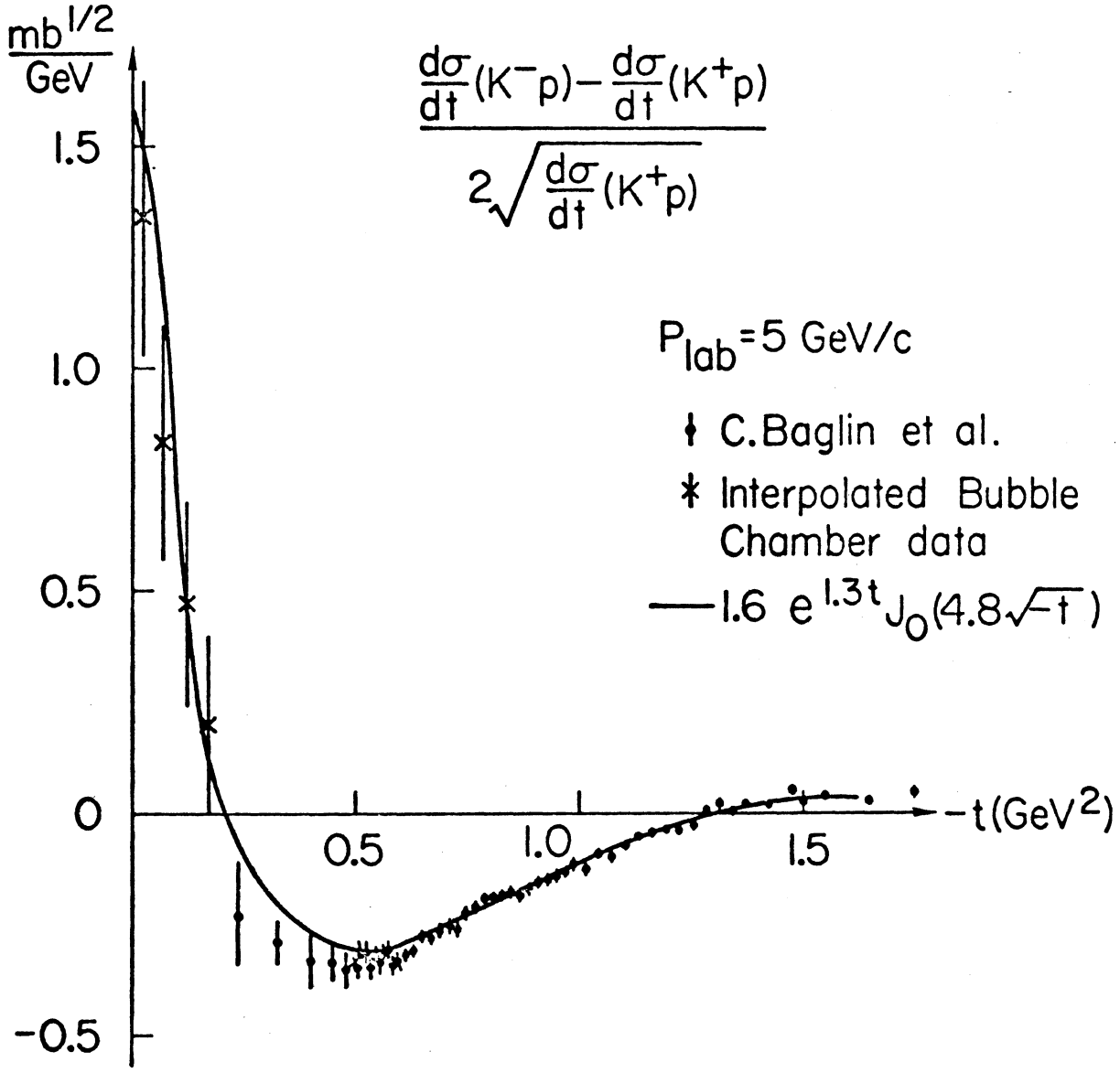
mb^1/2
GeV
1.5
1.0
0.5
0
-0.5
0.5
1.0
1.5
-t(GeV^2)
dσ/dt(K⁻p) − dσ/dt(K⁺p)
2√(dσ/dt(K⁺p))
P_lab=5 GeV/c
C.Baglin et al.
Interpolated Bubble Chamber data
1.6 e^1.3t J_0(4.8√-t)

FIG. 10

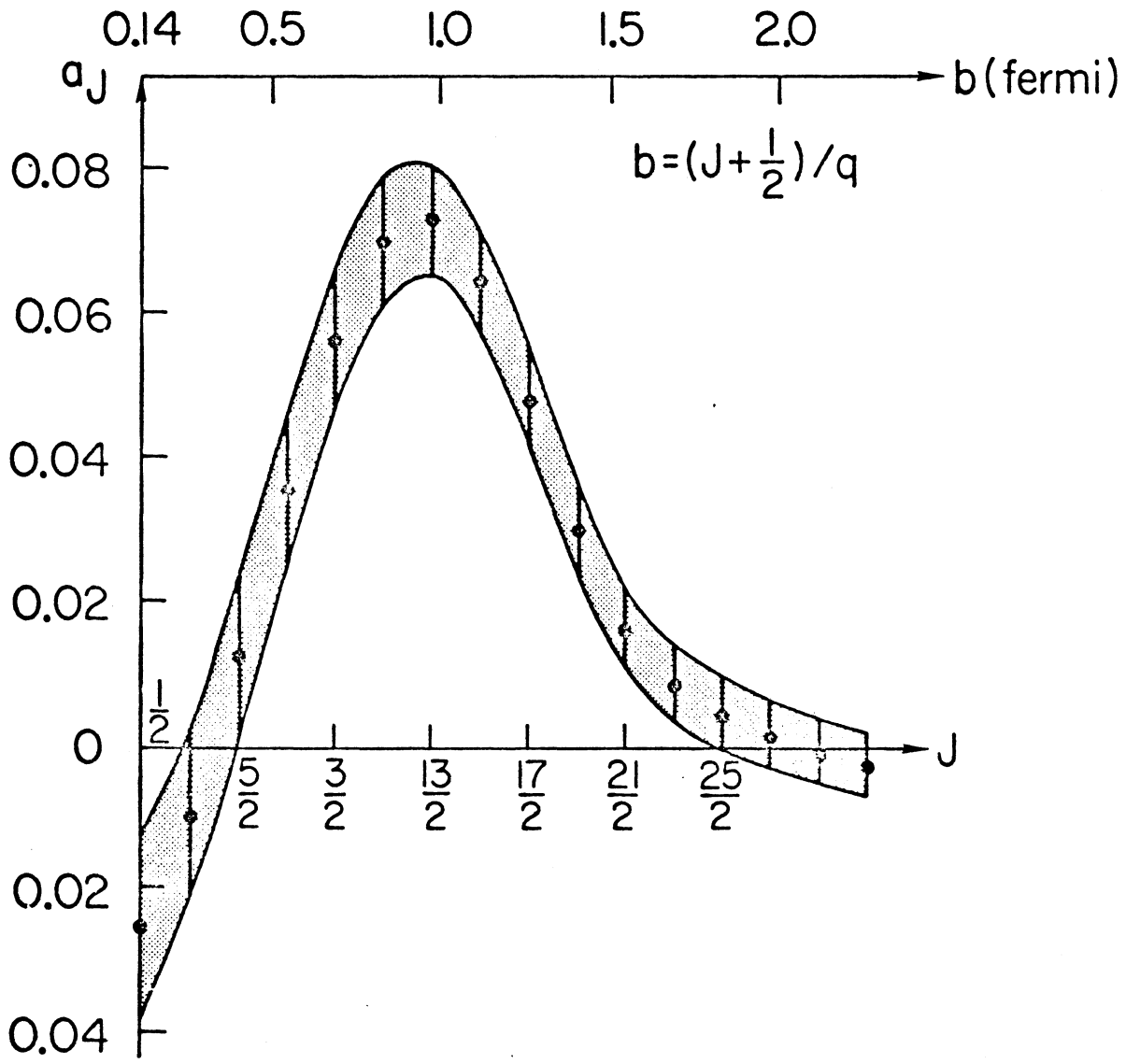
0.14
0.5
1.0
1.5
2.0
a_J
b (fermi)
$b=(J+\frac{1}{2})/q$
0.08
0.06
0.04
0.02
0
0.02
0.04
$\frac{1}{2}$
$\frac{5}{2}$
$\frac{3}{2}$
$\frac{13}{2}$
$\frac{17}{2}$
$\frac{21}{2}$
$\frac{25}{2}$
J

FIG. 11

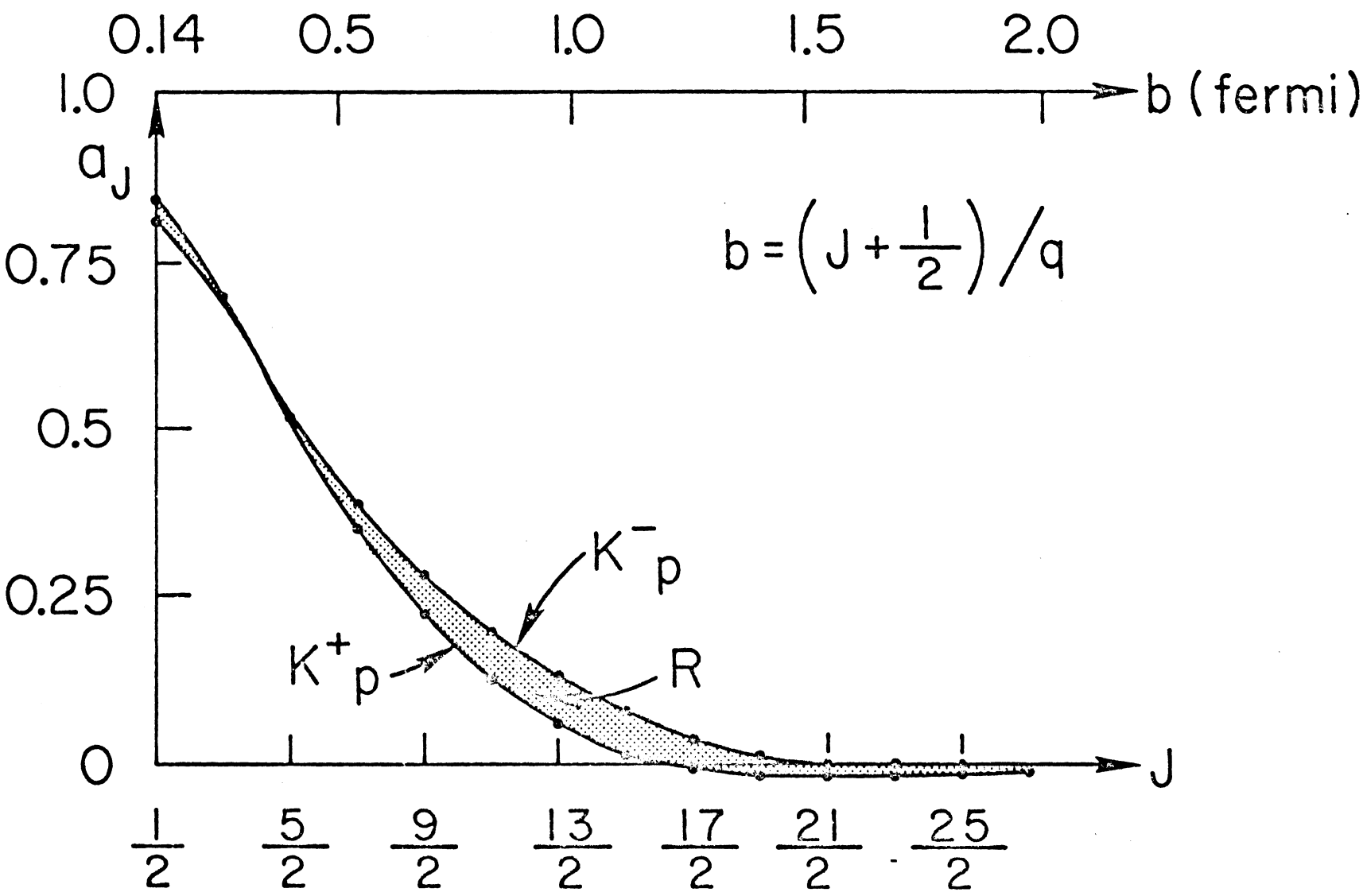
0.14
0.5
1.0
1.5
2.0
b (fermi)
1.0
a_J
0.75
0.5
0.25
0
$b = \left(J + \frac{1}{2}\right)/q$
K^-p
K^+p
R
J
$\frac{1}{2}$
$\frac{5}{2}$
$\frac{9}{2}$
$\frac{13}{2}$
$\frac{17}{2}$
$\frac{21}{2}$
$\frac{25}{2}$

FIG. 12

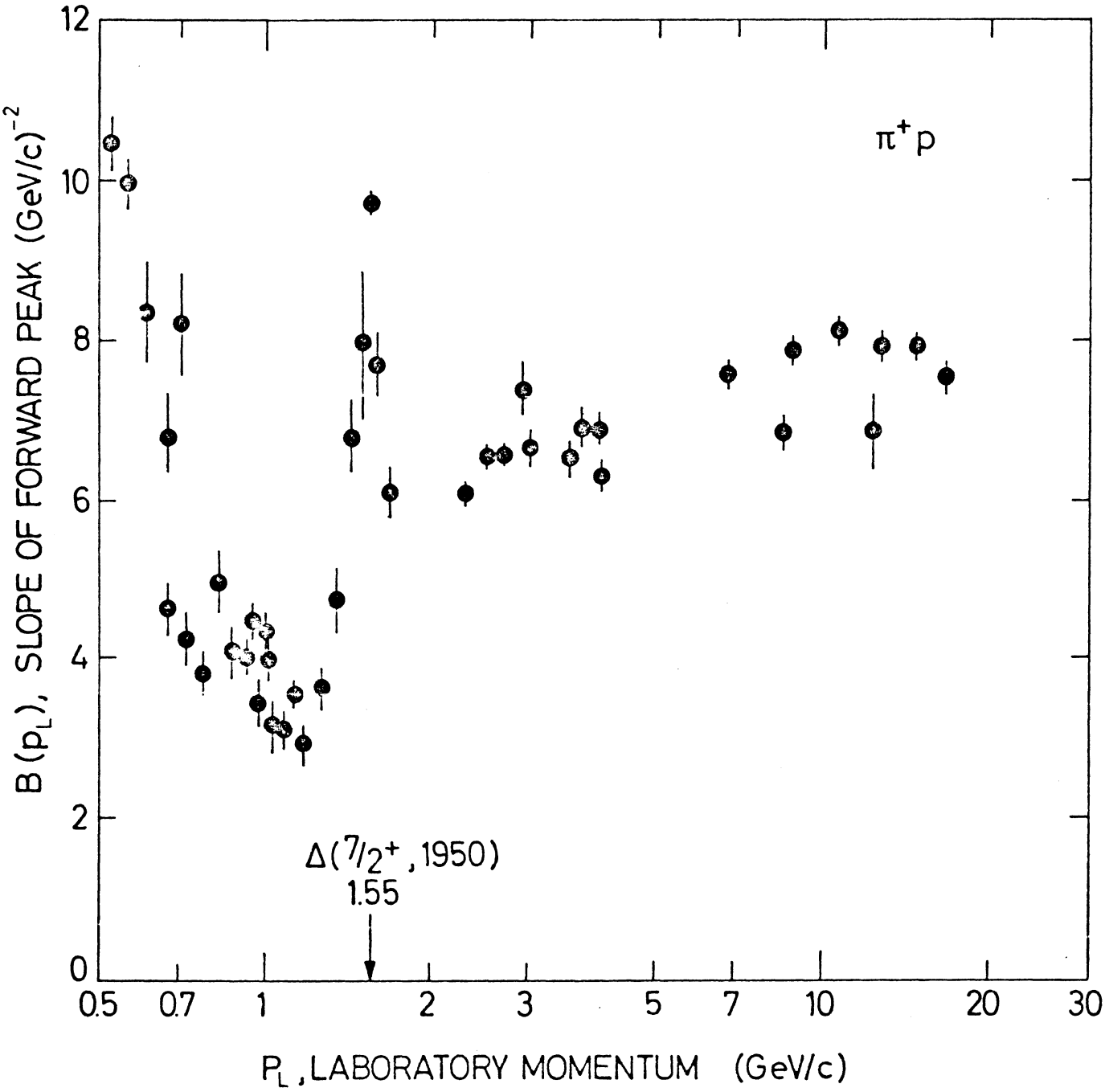
12
10
8
6
4
2
0
B (p_L), SLOPE OF FORWARD PEAK (GeV/c)^-2
π+p
Δ(7/2+, 1950)
1.55
0.5
0.7
1
2
3
5
7
10
20
30
P_L, LABORATORY MOMENTUM (GeV/c)

FIG. 13

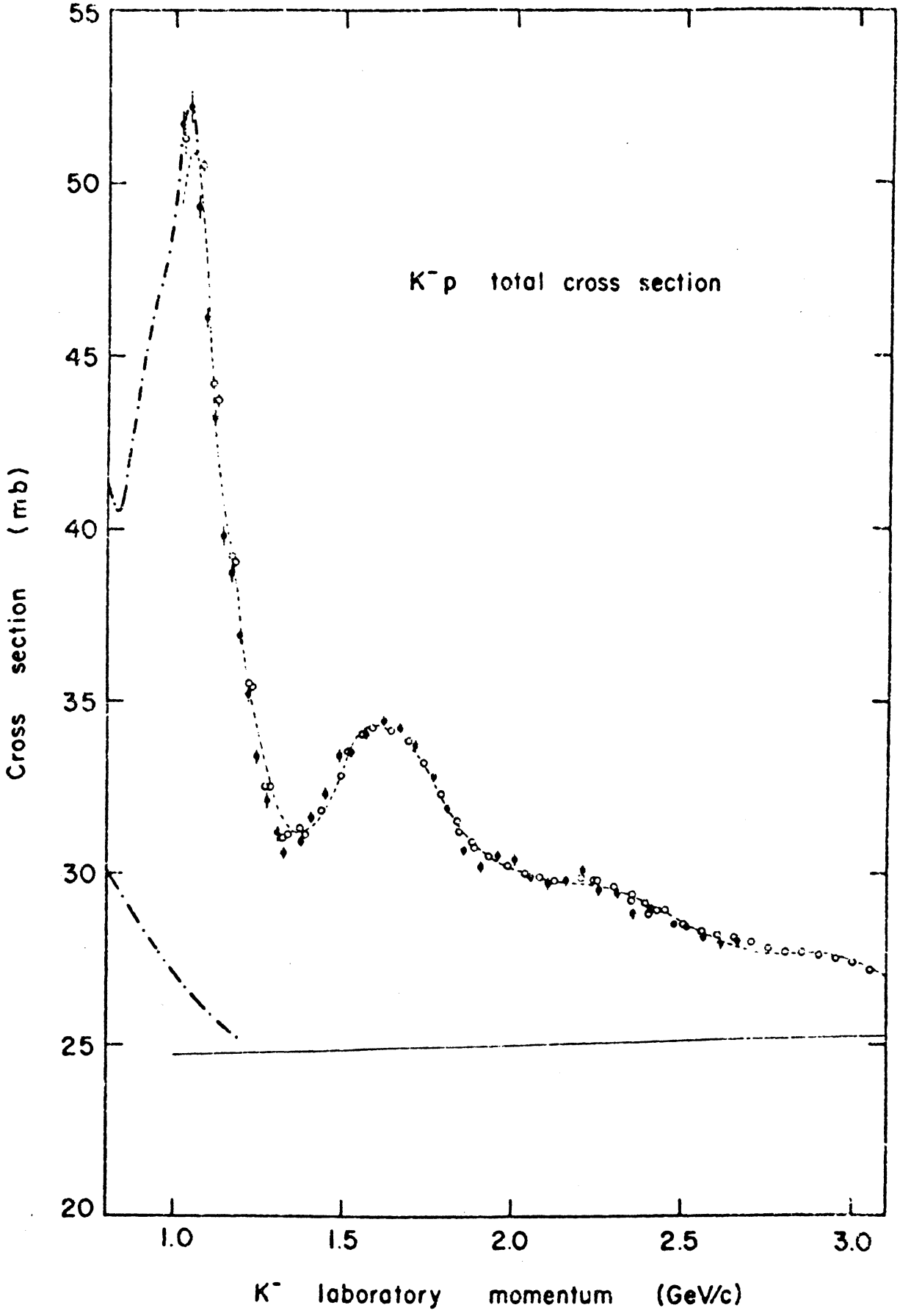
55
50
45
40
35
30
25
20
K⁻p total cross section
Cross section (mb)
1.0
1.5
2.0
2.5
3.0
K⁻ laboratory momentum (GeV/c)

FIG. 14

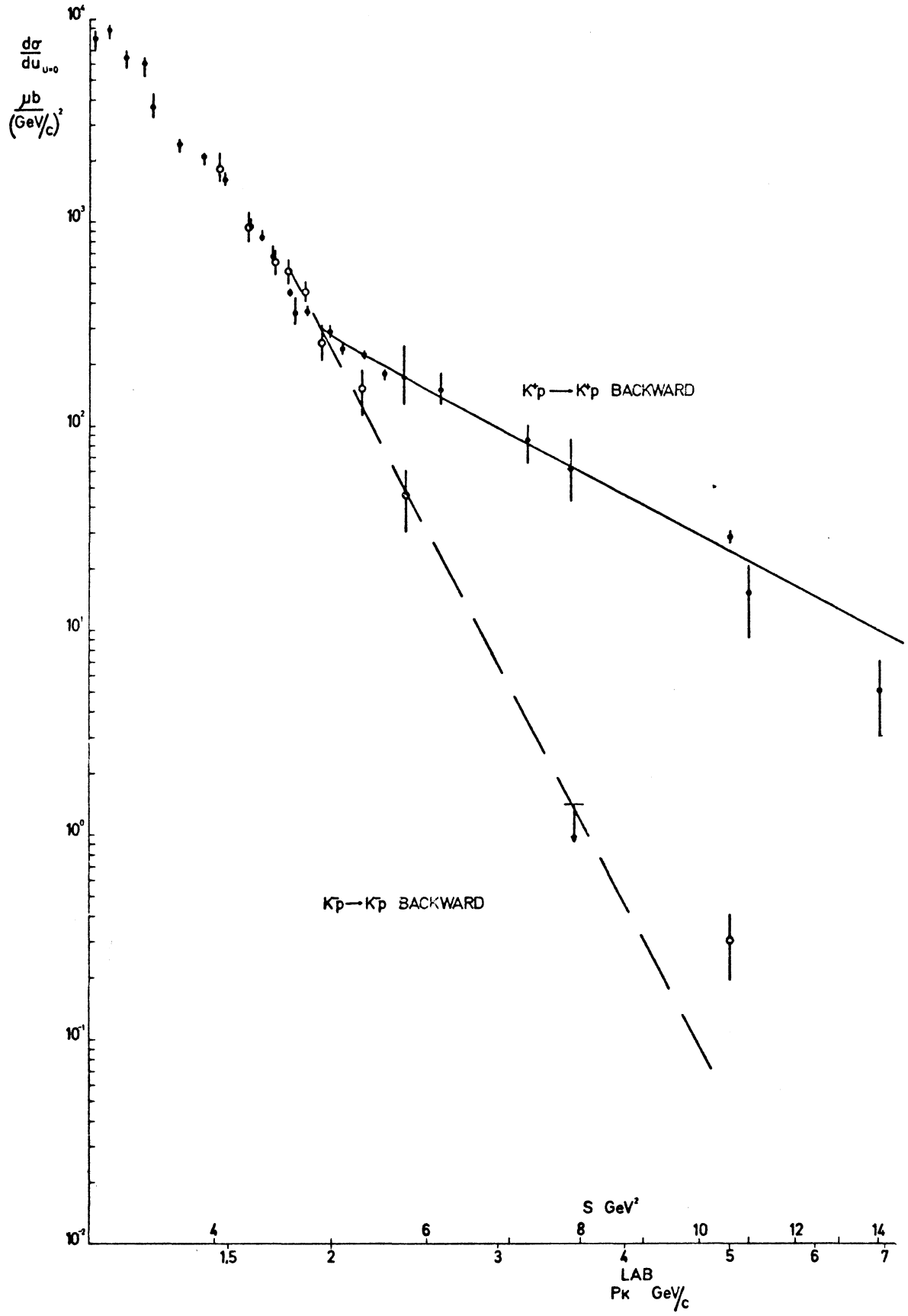
$\frac{d\sigma}{du}_{u=0}$
$\frac{\mu b}{(GeV/c)^2}$
10^4
10^3
10^2
10^1
10^0
10^{-1}
10^{-2}
$K^+p \longrightarrow K^+p$ BACKWARD
$K^-p \longrightarrow K^-p$ BACKWARD
S GeV²
4
6
8
10
12
14
1.5
2
3
4
5
6
7
LAB
P_K GeV/c

FIG. 15

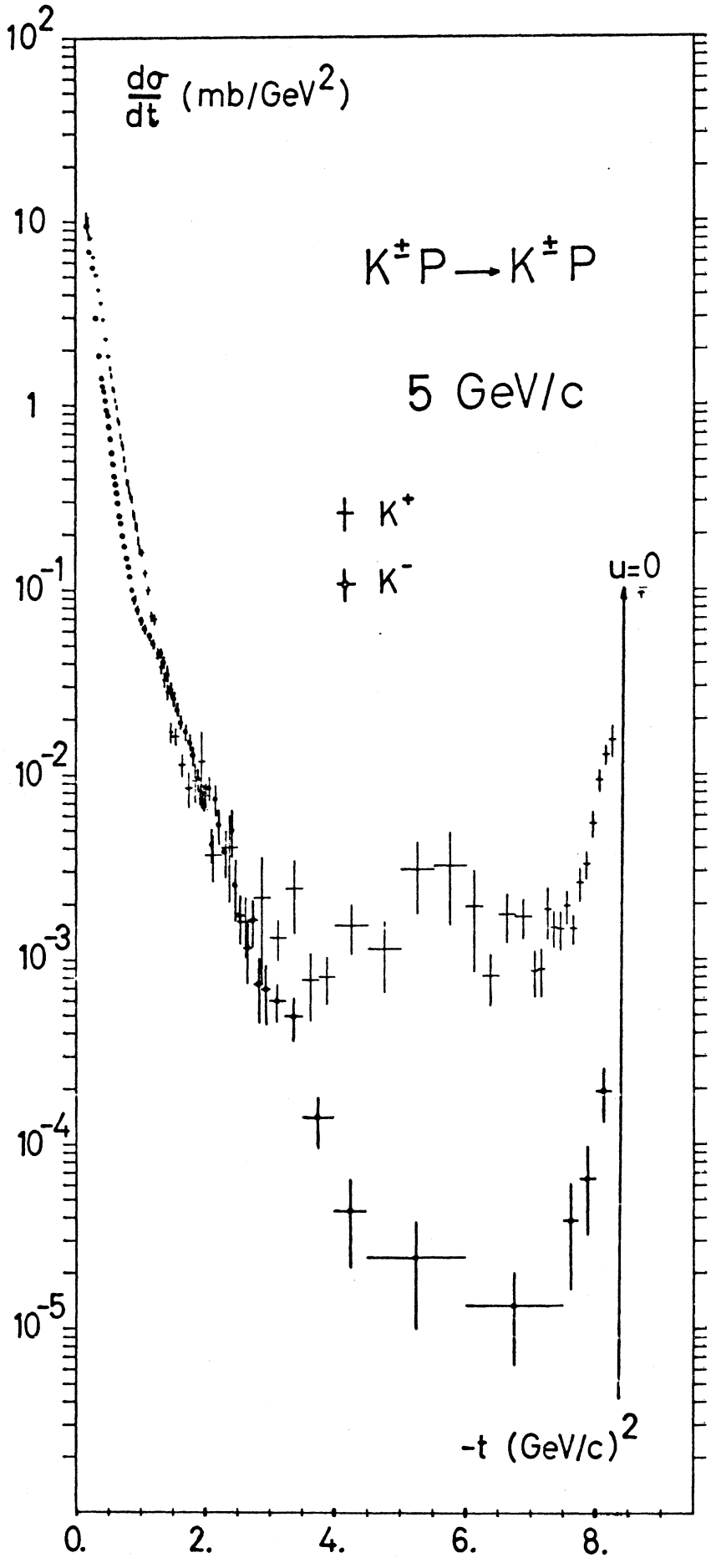
10^2
$\frac{d\sigma}{dt}$ (mb/GeV^2)
10
1
10^{-1}
10^{-2}
10^{-3}
10^{-4}
10^{-5}
$K^{\pm}P \rightarrow K^{\pm}P$
5 GeV/c
K^+
K^-
u=0
$-t$ (GeV/c)^2
0.
2.
4.
6.
8.

FIG. 16

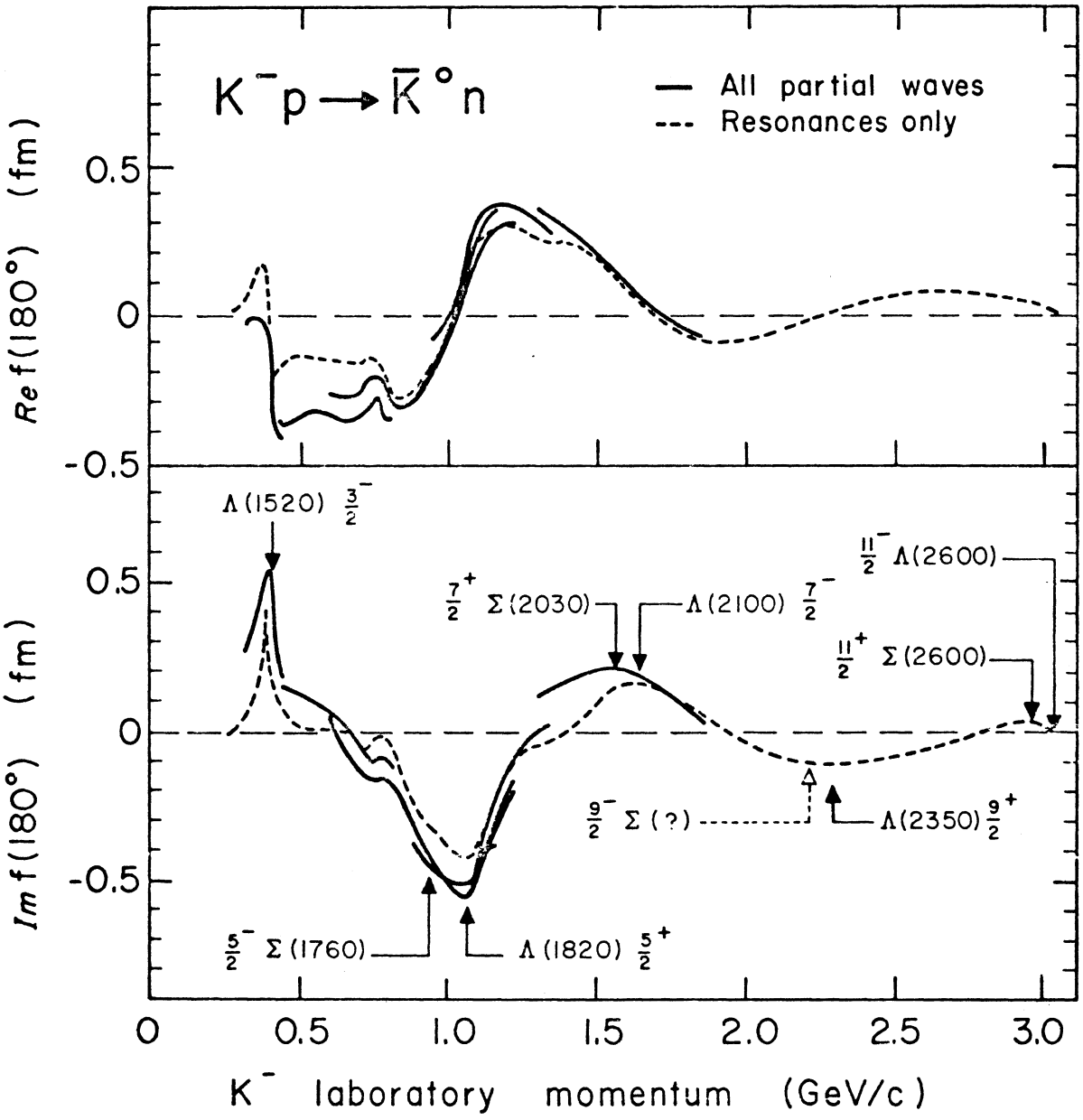
K⁻p → K̄°n
All partial waves
Resonances only
Re f(180°) (fm)
Im f(180°) (fm)
0.5
0
-0.5
Λ(1520) 3/2⁻
7/2⁺ Σ(2030)
Λ(2100) 7/2⁻
11/2⁻ Λ(2600)
11/2⁺ Σ(2600)
9/2⁻ Σ(?)
Λ(2350) 9/2⁺
5/2⁻ Σ(1760)
Λ(1820) 5/2⁺
0
0.5
1.0
1.5
2.0
2.5
3.0
K⁻ laboratory momentum (GeV/c)

FIG. 17